석사 학위논문
Master's Thesis

중력식 구조물을 이용한 해양원전의 개념 설계 및 내진해석

An offshore nuclear power plant mounted on gravity-based structures and its seismic performance

이 기 환 (李 起 煥 Lee, Kihwan)
기계공학부 해양시스템공학전공

School of Mechanical, Aerospace and Systems Engineering, Division of Ocean Systems Engineering

KAIST

2012

중력식 구조물을 이용한 해양원전의 개념 설계 및 내진해석

An offshore nuclear power plant mounted on gravity-based structures and its seismic performance

An offshore nuclear power plant mounted on gravity-based structures and its seismic performance

Advisor : Professor Phill-Seung Lee

by

Kihwan Lee

Division of Ocean Systems Engineering
School of Mechanical, Aerospace and Systems Engineering
KAIST

A thesis submitted to the faculty of KAIST in partial fulfillment of the requirements for the degree of Master of Science and Engineering in the School of Mechanical, Aerospace and Systems Engineering, Division of Ocean System Engineering. The study was conducted in accordance with Code of Research Ethics[1]

May. 23. 2012

Approved by

Professor Phill-Seung Lee

[1] Declaration of Ethical Conduct in Research**:** I, as a graduate student of KAIST, hereby declare that I have not committed any acts that may damage the credibility of my research. These include, but are not limited to: falsification, thesis written by someone else, distortion of research findings or plagiarism. I affirm that my thesis contains honest conclusions based on my own careful research under the guidance of my thesis advisor.

An offshore nuclear power plant mounted on gravity-based structures and its seismic performance

이 기 환

위 논문은 한국과학기술원 석사학위논문으로
학위논문심사위원회에서 심사 통과하였음.

2012 년 05 월 23 일

심사위원장 이 필 승 (인)

심사위원 정 형 조 (인)

심사위원 김 동 옥 (인)

MOSE
20104378

이 기 환. Lee, Kihwan. An offshore nuclear power plant mounted on gravity-based structures and its seismic performance. 중력식 구조물을 이용한 해양원전 개념 설계 및 내진해석. School of Mechanical, Aerospace and Systems Engineering, Department of Ocean Systems Engineering. 2012. 83 p. Advisor Prof. Lee, Phill-Seung. Text in English

Abstract

This paper proposes a new concept for an offshore nuclear power plant including its safety features. The design concept of the offshore nuclear power plant mounted on gravity-based structures (GBSs), which are widely used offshore structures, is proposed first. Based on the new concept, a large-scale land-based nuclear power plant model APR1400 with 1.4 GW electrical output is mounted on the GBS. A new total general arrangement (GA) and basic design principles that were used are described. Then, the safety features of the offshore nuclear power plant are discussed. A new emergency passive containment cooling system (EPCCS) and emergency passive reactor-vessel cooling system (EPRVCS) are proposed; their features of using seawater as coolant and safety features of against tsunamis, earthquakes, and marine collisions are also described. The proposed offshore nuclear power plant is safer than conventional land-based nuclear power plants and it has strong potential to provide great opportunities in nuclear power plant industries. Addition to the new design concept, dynamic behavior of GBS during earthquake implement with the consideration of soil-sea-structure interaction by ADINA finite element program. The analysis model is based on the SMART GBS type of ONPP. By changing of unit weight of GBS and friction coefficient between seabed and GBS as analysis variables, the dynamic response results is compared to clarify the acceleration response reduction effects at the GBS. A typical configuration of caisson-type GBS is used for analysis and three real earthquake records along with one harmonic excitation are imposed as base acceleration.

Keywords: Offshore nuclear power plant, gravity based structures, new total general arrangement (GA), emergency passive cooling system (EPCS), soil-structure interaction, base acceleration, horizontal acceleration response

Table of Contents

List of Tables

List of Figures

Chapter 1. Introduction

On March 11, 2011, an earthquake categorized as 9.0 M_W on the moment magnitude scale occurred off the northeast coast of Japan and a tsunami attacked the northeast shore after the earthquake. Resulting from these natural events, the Fukushima Daiichi nuclear disaster occurred and it alerted society to the risks of nuclear power plants again. Even though nuclear power plants have catastrophic risks, they will not be given up because nuclear power has a small CO_2 emission, a relatively low fuel cost, and high fuel efficiency. Therefore, in order to use nuclear power continuously and safely, technology development for enhanced safety is essential for future nuclear power plants.

One potential solution for using nuclear power safely could involve moving the conventional nuclear power plant (NPP) from land to ocean in an effort to enhance the safety of conventional NPPs. Generally, this type of nuclear power plant is called an offshore nuclear power plant (ONPP) because its operating location is in the ocean. ONPPs have several advantages.

- ONPPs can be transportable. This valuable feature could result in higher fabrication quality and shorter construction period.
- Since ONPPs are located far from residential areas, they may have a positive influence on the public acceptance of NPPs.
- ONPPs have ample cooling water using the seawater on which they are located. Therefore, sufficient cooling water can be used if a beyond design accident occurs, such as the Fukushima disaster.
- The offshore solution may also be attractive with regard to future expansion that can be achieved through allocating space on the first development or by adding another structure or facilities that may be installed adjacent to the existing facilities, without concern for acquiring land or receiving negative public feedback.

Based on the strengths discussed, many countries have developed several concepts and ideas of ONPPs previously, and the ONPP research continues now. In the beginning of the 1950s, the USA and USSR began to develop floating nuclear power plants. Recently, Russia's first floating NPP was scheduled to be completed and is expected to be operational in 2013; furthermore, the French undersea nuclear power reactors that are located around the coast of France are examples of the heavy investments in nuclear

power that have been made by the French government. Russia's floating NPP uses two 35 MW reactors derived from those used in Russian icebreakers. Since the floating type NPP is easily affected by severe ocean environments, it should be operated in calm sea, such as a port inside of breakwater barriers. The French undersea ONPP is difficult and dangerous from the perspective of control and maintenance. Both types of ONPPs can mount nuclear reactors with relatively small capacity

The key idea of this study is that we adopt gravity-based structures (GBSs) for ONPPs, which have been widely used for many offshore plants. GBSs are typically made by steel reinforced concrete in dry dock and tugged to destination site after floated; that is, GBSs are transportable. During operation, they sit on seabed and bear all the external loadings by their self-weight (gravity). A common GBS application is offshore oil platforms, but recently GBSs are also being used for wind turbines and LNG terminals. The advantages and disadvantages of floating, GBS, and submerged ONPPs are summarized in Table 1. It is important to note that, being different from floating and submerged types of NPP, GBS can heavy large-scale NPPs and provide land-like environments for topside facilities. This paper presents the concept and key ideas of the GBS type ONPP in detail.

Table. 1. Advantages and disadvantages of various types of ONPP

Floating	
Advantages	- Moveable - Relatively cost effective compared with GBS
Disadvantages	- Easily affected by ocean environment - Difficult to control operating system
GBS	
Advantages	- Durable - Stable in the ocean environment - High performance of construction work - Securing safety features in case of marine collisions - Buoyancy control of the structure
Disadvantages	- Limitation of water depth - Lower cost effectiveness
Submerged	

Advantages	- Relatively free from the limitations of water depth - Invisible
Disadvantages	- Difficult to control and maintain the entire system - Requires relatively long and expensive cabling to land - Relatively small electricity generation capacity

To effectively utilize the plentiful source of cooling water from the ocean, new concepts for the emergency passive cooling system (EPCS) are suggested: emergency passive containment cooling system (EPCCS) and emergency passive reactor-vessel cooling system (EPRVCS). This work proposes the concept systems for the GBS type ONPP to enhance the existing EPCS that is originally designed for land-based NPPs. The EPCCS and EPRVCS use the natural differential head pressure between the ballast compartments filled with ballast water and the inside of the containment as a driving force for passive system. In addition, the general discussions on the safety features of the GBS type ONPP against tsunamis and marine collisions are addressed.

Earthquakes have been a most severe threat for land-based NPP and, of course, it is the same case for ONPP. However, GBS based NPP have totally different structural features and subjected to different surrounding environments. It is importantly required to address the general discussions in the concept design phase. Also, it is necessary to discuss on the additional safety features of the GBS type ONPP against tsunamis and marine collisions.

Addition to the general discussion about seismic performance of GBS based ONPP during earthquake in a concept design phase, we need to investigate the dynamic response of GBS during earthquake because GBS is relatively less affected by ocean environment due to its massive volume and weight, but it is easily damaged under severe earthquake because GBS bottom directly contact with seafloor.

Usually, bottom of GBS is fixed to the floor with skirt foundation, but during the extreme earthquake, the skirt below the base slab is designed to yield. After yielding of skirt due to extreme earthquake, GBS is slightly sliding on the seafloor. In this phase, the coefficient of friction between GBS bottom and seafloor and total weight of GBS are acting as governing parameters of sliding motion of GBS. This phenomenon is similar to the pure frictional base isolation system.

In this study, total weight of GBS and friction coefficient are regarded as analysis variables for dynamic response analysis of GBS type ONPP during earthquake. GBS has ballasting system, which control the weight of ballast compartment using water or sand with the purpose of launching, towing and settling down of GBS to the target site. By controlling of total weight of GBS using ballasting system, the dynamic response of GBS can be changed. The fictional forces mobilized at the sliding bottom are assumed to have the ideal Coulomb-friction characteristic. Under the assumption of ideal Coulomb-friction, frictional forces are governed by superstructure`s total weight and coefficient of friction. To clarify such dynamic response and frictional base isolation effects according to change of unit weigh and coefficient of friction during earthquake, dynamic response analysis of GBS during three real-earthquake and one harmonic ground motion have been conducted. Earthquake waves, acting on the GBS base slab directly and cause an oscillatory motion of the whole structure. Consequently, vibration is occurred at the structural component, mechanical and electrical equipment and it causes damage and collapse on structure and malfunction of system which situated inner and topside of GBS type ONPP.

To analyze dynamic behavior of GBS during earthquake, including soil-sea-structure interaction, in this study, dynamic response of GBS is calculated by ADINA finite element program. Comprehensive seismic finite element analysis was used to determine the overall dynamic behavior of the entire fluid-structure-soil interaction (FSSI) system.

The specific aims of the present research can be summarized as: (1) to present a FE model for FSSI FE model and analysis of dynamic response of GBS using ADINA finite element program, (2) to study the dynamic acceleration response according to change of total weigh of GBS. This achieved by comparing the response of FSSI system under harmonic and three selected real earthquake ground motions with consideration of interaction between frictional forces to the corresponding response without interaction; GBS bottom is fixed to the seafloor, and (3) to investigate the influence of friction coefficient on correlation between frictional force and dynamic acceleration response according to change of friction coefficient. In addition, dynamic response is investigated comparing between weight change and coefficient of friction change.

In this paper, a new concept for nuclear power plants is presented based on the ocean environment in order to overcome the safety limitations of conventional land-based

NPPs and related social problems. Also, the safety features for the concept and dynamic response analysis of GBS during earthquake are presented.

Chapter 2. Design Concept of the ONPP

Being different from the floating and submerged ONPP concepts, a GBS type ONPP is proposed. The GBS is a rectangular structure for ease of construction and instead of developing a new design for the plant layout and nuclear reactor systems, the existing plant layout and system of the land-based NPP APR1400 is used. However, the total GA of the APR1400 must be appropriately modified because the entire plant building, site facilities, and other systems need to be separated and mounted onto GBS modules. In order to enable this, modularization of the APR1400 components involving the site facilities is proposed with consideration of the functions of the buildings and facilities, and systematic correlation from the dual viewpoint of a structural and systematic approach. In this section, based on the governing design parameters, we describe the key concept, a new total GA and concept design of GBS type ONPP.

2.1 Governing design parameters for the concept development and design requirements of the GBS type ONPP

Recently, several specific guidelines from certifying companies have been issued that relate to offshore floating and GBS production (Waagaard et al., 2004); furthermore, the public design regulations and demand of nuclear engineering have also been well developed. Thus, in order to develop GBS type ONPP, the design requirements must be satisfied and several specific guidelines must be followed for both nuclear power plants and offshore structures. However, for the present phase, the design requirements and regulations cannot be precisely met and followed because there have not been specific design requirements and regulations for NPPs mounted on GBSs; furthermore, previous studies and research does not exist for GSB type ONPPs. Thus, in this study, instead of attempting to satisfy both offshore structure and NPP regulations and guidelines, the focus has been on the common and essential design requirements of the GBS type ONPP. Therefore, in the conceptual phase, the key design parameters of the GBS type ONPP are proposed based on the established material (Haug et al., 2003; Waagaard, 2004), including the following aspects:

- Volume requirements of the NPP building and facilities
- Main nuclear power system requirements
- Operability requirements and radiation shielding ability in various accident scenarios
- Current drift
- Construction concerns specific to nuclear power
- Soil conditions and water depth
- Construction restraints as draft limitations during the tow-out, installation, and construction of the yard/dry-dock limitations
- Any constraints at the offshore location
- Balanced weight distribution

Generally, the soil condition and water depth are the dominant parameters for the construction and installation of GBSs. In particular, the total weight of NPP's main buildings and systems are massive, thus a weight-balanced arrangement of the buildings is required in order to prevent differential settlement and the selection of a construction site demands great caution. To prevent the blending of the intake and discharge circulation water, and prior to fixing the installation direction of the GBS type ONPP, research on the current drift is essential and must be reflected in the design parameters.

2.2 Key concepts of the GBS type ONPP

The GBS is a support structure which retaining its position by massive self-weight; GBSs are usually used as an offshore oil platform and foundation structures in the ocean and are constructed by steel reinforced concrete. The concrete material has characteristics in relation to fire resistance, radiation shielding ability and durability against external impact loading. Recently, GBSs are also being used for offshore wind power plants. Recent example of a GBS offshore structure is the Adriatic LNG Terminal (Ludescher et al., 2011). The first offshore liquefied natural gas (LNG) terminal using a concrete GBS that was successfully fabricated which are located 15 km away from the Italian coast in September 2008.

The key concept of the GBS type ONPP is the use of the GBS as a container and support structure similar to that used in the Adriatic LNG Terminal and the use of a modular design for the ship fabrication methods at an on-site factory facility. When the fabrication and assembly of the GBS and NPP modules are completed, the GBS

modules are launched and towed by tugboats to the ONPP site; then, the modules are placed on the seabed at the target site using a ballasting system. The detailed procedures are shown in Figure 1. The four basic steps of this procedure are listed below.

Step 1. Fabrication of several GBS modules in dry dock, modularization of NPP`s facilities and preparing of the ocean site are proceeding at the same time.

Step 2. Fabricated modules based on the new total GA are constructed on the GBS. The modular NPP is built at an on-site factory and the modules are mounted on the GBSs. In this step, the first inspections and testing of the modularized facilities are required prior to launching.

Step 3. The floatable and moveable GBS type ONPP is towed to the ocean site using tugboats. Using a ballasting system with a concrete double hull, the GBS draft control and stabilization are possible.

Step 4. Nuclear fuel loading and system testing procedures are implemented by the operator and additional constructions of the top-side facilities are undertaken in parallel. Finally, the ONPP is ready to supply electricity to the land.

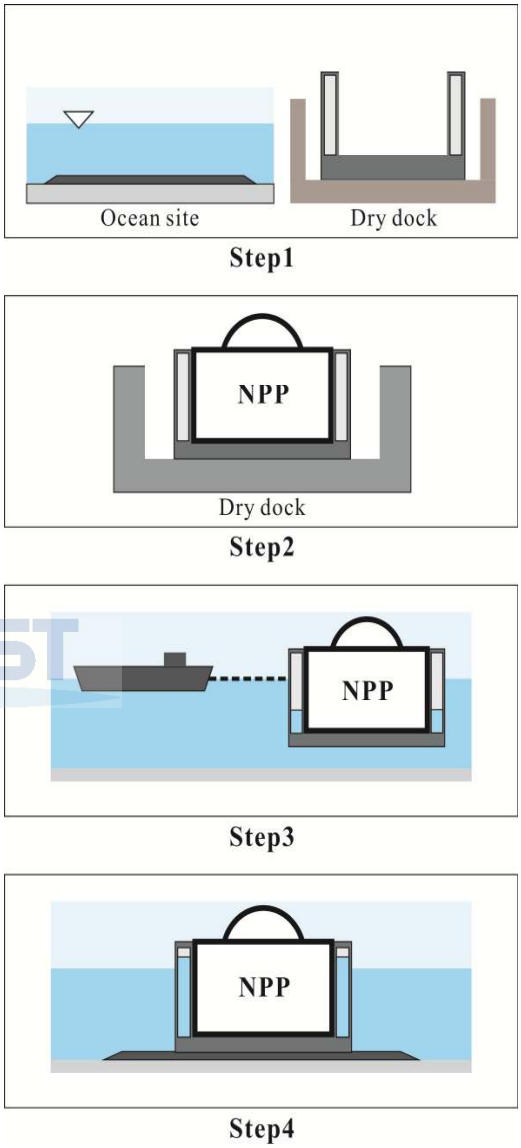

Fig. 1. The key concept and installation procedures of the GBS type ONPP

2.3 New total GA of the GBS type ONPP

Previous research on the modularization of a land-based NPP proposed the land-based NPP design-fabrication approach to increase the quality and reduce the costs of future

plants. This research primarily focused on nuclear-related buildings and their associated systems (Lapp & Golay, 1997). However, in the present study, with the purpose of properly separating overall building`s and facilities of APR1400 into the several GBS caissons, the modularization method is used for not only the reactor and auxiliary building, but also other land-based NPP site facilities and buildings.

The modularization design method is not discussed in this study because the purpose of this study is proposing a new concept of GBS type ONPP. This paper is the first research of combining both fields of offshore structures and nuclear engineering, hence it is difficult to follow and apply public design regulations and requirements; furthermore, as mentioned in Section 1, the GBS type ONPP is developed based on the land-based NPP APR1400. That is, the established GA of the APR1400 is used, in particular, the nuclear-related buildings and their associated systems. Also, the APR1400 is the most recently approved Korean NPP model, and the nuclear-related buildings and their associated systems are already modularized. In this paper, the meaning of modularization corresponds to all NPP buildings and site facilities. The APR1400's GA and pipeline arrangements are shown in Figure 2 and the corresponding legend is given in Appendix A.

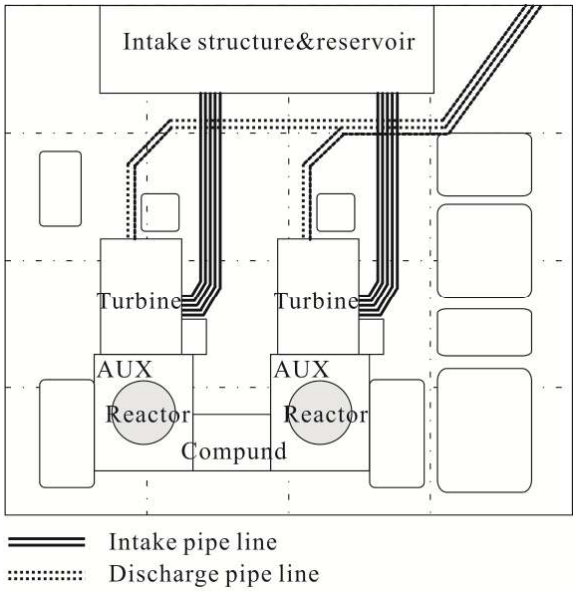

Fig. 2. APR1400 NPP building component, facilities, GA, and pipeline arrangements

In order to modularize the land-based NPP APR1400 model, the design factors must be

examined thoroughly; the design factors include the physical connectivity, nuclear and non-nuclear buildings, pipeline arrangement, building weight, building placement symmetry, and availability of fabrication and maintenance. The new total GA should be developed considering these design factors. In this study, the meaning of the new total GA is not limited to the turbine building, compound building, reactor containment building, and reactor auxiliary building; rather, it includes all facilities and buildings of the APR1400.

2.3.1 Nuclear and non-nuclear areas

In this section, based on the APR1400 model GA, a new total GA for the GBS type ONPP is proposed. Firstly, the APR1400 building components are categorized into nuclear and non-nuclear buildings. A detailed differentiation of the nuclear and non-nuclear areas is shown in Figure 3. The shaded sections indicate a nuclear area and the unshaded sections indicate a non-nuclear area.

The nuclear buildings include the following:

- Reactor auxiliary building
- Reactor containment building
- Waste process building
- Fuel handling building

The non-nuclear buildings include the following:

- Turbine generator building
- Intake structure
- Control building
- Compound building
- Water treatment building
- Accommodation and other warehouse buildings

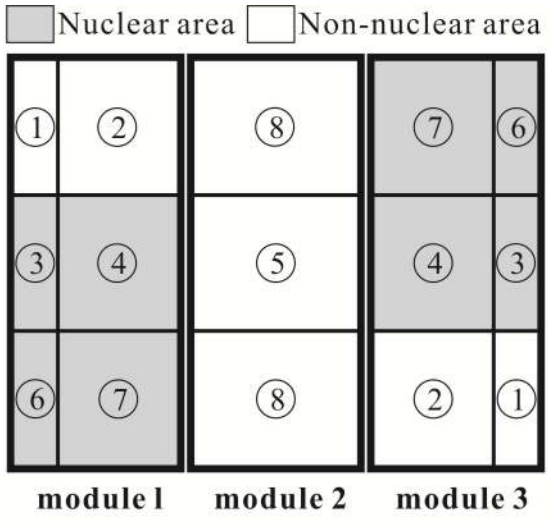

Fig. 3. New total GA of the GBS type ONPP with differentiation of the nuclear and non-nuclear areas

2.3.2 Modularization of the NPP buildings and facilities

In this section, based on the APR1400 GA and the nuclear and non-nuclear area categories, the element groups are suggested and a new total GA for the GBS type ONPP is constructed. Before modularizing of the total NPP components, the building functions and NPP system assignments must be considered. The GBS type ONPP consists of three GBS caisson modules and each module is composed of up to six element groups (with a total of eight different groups; some groups are duplicated). Figure 3 shows the arrangement of the GBS type ONPP's three modules and fifteen components. The details and functions of each group are as follows.

① Group 1 includes the following elements:

- AAC D/G building
- Auxiliary boiler building
- Auxiliary boiler fuel oil storage tank
- Fresh water storage

This group has no direct correlation with the reactor building system and safety system and it also contains flammable facilities, materials, and fresh water storage, so it must remain apart from the reactor building systems.

② Group 2 includes the following elements:

- Turbine generator building
- Main transformer
- Standby auxiliary transformer
- Unit auxiliary transformer
- Spare main transformer
- Lube oil storage tank and centrifuge house.

The turbine shaft must be nearly located in the center line of the reactor containment and auxiliary building in order to protect the reactor building systems from the turbine missile strike zone in case the turbine blades are destroyed as shown in Figure 4. The electric power systems are correlated with the turbine generator building; thus, the main, standby, and spare transformer and switchgear buildings must be located in the same group.

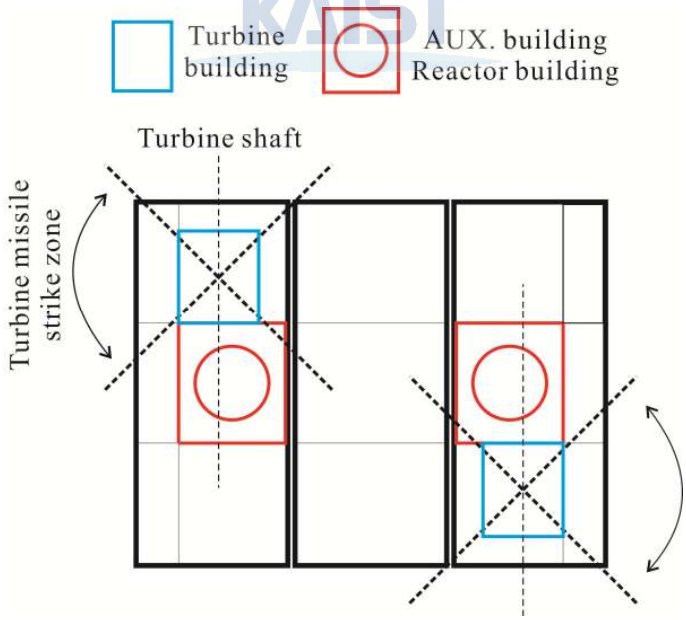

Fig. 4. Layout of the turbine and reactor buildings in order to protect the reactor building from the turbine missile strike zone

③ Group 3 includes the following elements:

- Reactor make up water tank,
- Hold-up tank, and
- Boric acid storage tank.

The reactor make-up water system and hold-up tank must be located next to the reactor building systems because these facilities have heavy physical connections with the reactor building systems.

④ Group 4 includes the following elements:

- Reactor containment building, and
- Auxiliary building.

The auxiliary buildings are designed as a quadrant shape, allowing it to wrap around the containment building and divide the safety systems into four sections as shown in Figure 5. Through the quadrant shape safety systems, the auxiliary buildings are able to manage conflagration, flooding, and other external accidents.

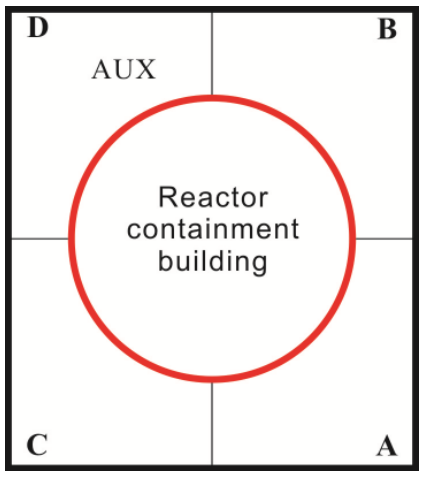

Fig. 5. Layout of the auxiliary building and reactor containment building

⑤ Group 5 includes the following elements:

- Office building,
- Compound building, and

- Control building

For the convenience of controlling and operating the ONPP, the office building, control buildings and compound building are positioned at the center of GBS Module 2.

⑥ Group 6 includes the following elements:

- the discharge pond and facilities.

The discharge pond is located next to the water treatment systems, allowing easy drainage of the water from the ONPP and also avoiding interference with the intake structure. The discharge pond and facilities must be located far away from the intake structure and should have a different emission direction to that of the water intake direction.

⑦ Group 7 includes the following elements:

- Wastewater treatment facility,
- Fire pump and water/wastewater treatment building,
- Caustic and acid storage tank,
- Cooling tower,
- Chlorination building, and
- Sodium hypochloride holding tank.

In order to easily manage the used water and chemical waste that are generated from the power plant, the sanitary water treatment facility and wastewater treatment facility should have a physical connection with the reactor building systems.

⑧ Group 8 includes the following elements:

- Intake structure and reservoir,
- CCWHX building,
- ESW intake structure,
- Sanitary water treatment facility,

- Accommodation, and
- Refuge

In order to secure and store the circulation cooling water for the facilities in the ONPP, this subcategory requires sufficient space for the reservoir systems and water treatment facilities. The ESW intake structure and CCWHX buildings have physical connections with the turbine generator building and reactor building systems, both directly and indirectly; hence, this subcategory should be connected with the turbine generator building. The intake structure and reservoir systems should be connected with the accommodation and office building in order to supply potable water for the operators and workers. The accommodation is essential for the operators and workers inhabiting the ONPP; it is also a populated area, so it must be separated from GBS Module 1 and Module 3 (as shown in Figure 3). For the event of emergency, workers escape from GBS as soon as possible. Therefore, the location of refuge is positioned in GBS module 2 and involved in group 8.

2.3.3 Symmetric structure arrangement with the weight balance

In case of land-based NPPs, the main buildings and facilities have their own independent foundation, but ONPPs share foundations because the reactor building, turbine generator building, and other facilities are mounted onto the same GBS module. Hence, the total weight balance is a very important design parameter when developing a new total GA in order to prevent differential settlement. Each main building`s total weight information is an essential design parameter for developing a new total GA. Table 2 presents the main buildings' weight information for the APR1400 model NPP.

Table. 2. Specific weight information of the APR1400

APR14000 weight information	
Legend	Weight (ton)
Reactor building	480,000
Auxiliary building	540,000
Compound building	76,000
Turbine generator building	440,000
Other facilities	200,000

For the GBS Module 2, Group ⑧ is symmetrically located at both ends and Group ⑤ is located in the center of GBS Module 2. Consequently, GBS Module 2 has symmetric arrangement with weight balance. Group ④ and Group ② are the heaviest components of GBS Module 1 and GBS Module 3, respectively. Group ④ should be located the middle of GBS Modules 1 and 3 because it contains the auxiliary and reactor buildings. If Group ④ is located at the identical both ends of the GBS module, it could cause differential settlement. Group ② is the second heaviest area of GBS Modules 1 and 3. Unlike Group ④, Group ② should be placed in the ends of the GBS module, but it should be located opposite ends side of GBS Modules 1 and 3. If Group ② is placed at the same end of GBS Modules 1 and 3, it could cause differential settlement. Thus, the new general GA has a diagonally symmetric arrangement and also the center of the mass exists on a diagonal axis as shown in Figure 6.

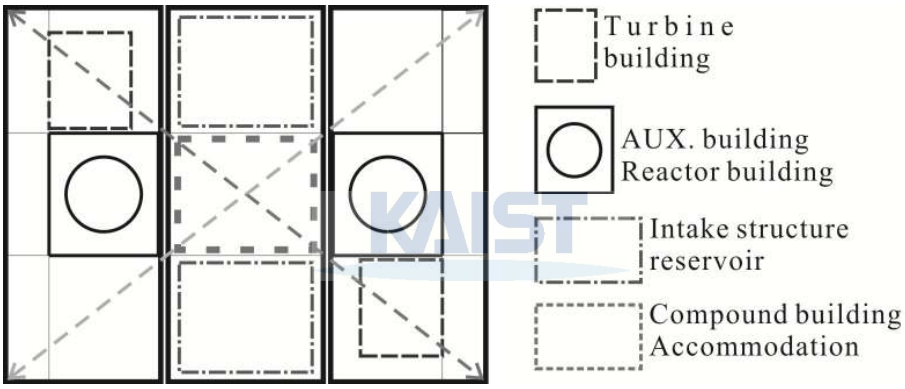

Fig. 6. Diagonally symmetric arrangement of groups considering the weight balance

2.3.4 Pipeline arrangement of the GBS type ONPP

A new total GA for the GBS type ONPP is proposed based on the design parameters and with feasibility considerations which are suggested in the previous section. As the arrangement of the NPP's components is rearranged, the NPP's pipeline arrangement must also be rearranged according to the new total GA. The changed pipeline arrangement of the GBS type ONPP is shown in Figure 7. In contradistinction to the NPP pipeline arrangement, the GBS type ONPP's pipeline arrangement is relatively simple and the overall pipeline length is shorter than that of the NPP. In case of the APR1400, the intake structure and reservoirs are located approximately 200 m from the turbine building, and the cooling water discharge pond is located far away from the power plant site in order to prevent the intake and discharged cooling water being mixed.

Thus, the overall pipeline length is very long. However, the GBS type ONPP's turbine building group is located next to the intake structure and reservoir group, so the intake pipeline is short. Furthermore, because the cooling water discharge pond and turbine building are positioned in the same GBS module, the overall discharge pipeline length can be reduced. Consequently, the GBS type ONPP is more economical in terms of pipeline length. However, the intake structures and discharge ponds are positioned within the GBS type ONPP, the risk of blending the circulating cooling water is relatively high. In order to prevent mixing the circulating cooling water, the current drift must be researched and considered prior to determining the installation direction of the GBS. If necessary, an extension of the discharge pipeline to a location further away or an additional discharge pond located elsewhere can reduce the risk of the circulating cooling water being mixed.

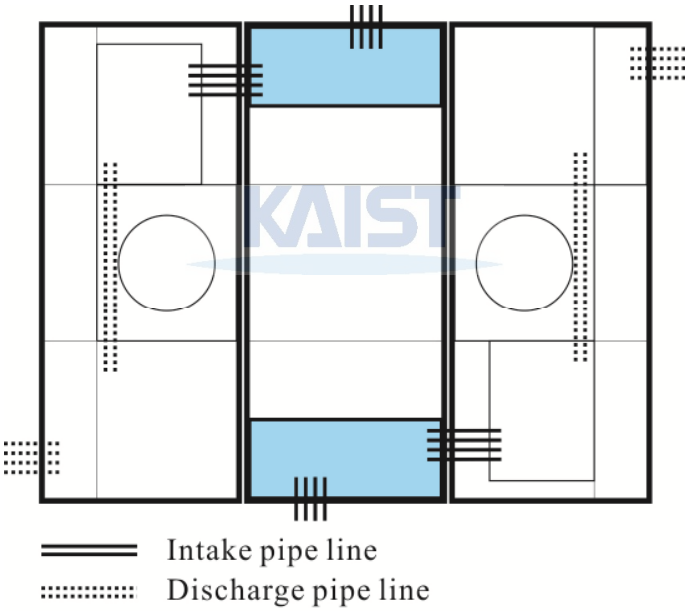

Fig. 7. Pipeline arrangement of the GBS type ONPP

2.4 Concept design of the GBS type ONPP

In this section, all main buildings and other facilities of the NPP, as modularized in Section 2.3.2, are arranged with three GBS modules based on the considerations explained in Sections 2.1 and 2.3.

The design philosophy of the GBS type ONPP is compactness and safety. Through the modularization and rearrangement of site facilities and pipeline, the total nuclear power

plant site area can be reduced. The GBS type ONPP has overall dimensions of 270 m (L), 330 m (W), and 53 m (H), and each GBS concrete caisson module is 270 m (L), 110 m (W), and 53 m (H) with symmetric arrangement. The original site area of the APR1400 is 225,000 m^2 and the ONPP site area is 89,100 m^2; thus, the total area of the GBS type ONPP is reduced by 60% (135,000 m^2) compared with the original NPP site area as depicted in Table 3.

Table. 3. Site area comparison data between the NPP and ONPP

	Site dimension (m)	Total site area (m^2)
NPP	500 × 450	225,000
ONPP	270 × 330	89,100

In order to settle down GBS to the seafloor, ballasting and deballasting systems are essential. The GBS has a concrete double bottom and concrete double walls all around that act as ballasting systems; the double walls can also increase the durability of the GBS against boat and floating object collisions. The safety features of the GBS are demonstrated in Section 3 in more detail.

The target water depth of the GBS type ONPP at the construction site is 30 to 35 meters. The suggested height of the GBS is 53 m in this study, which allows 18 to 23 m of freeboard to be secured. The 18 to 23 m of freeboard is sufficient to effectively prevent "green water" on the top of the GBS under storm and severe weather conditions. The detailed dimensions and design of the concrete caissons are shown in Figures 8.

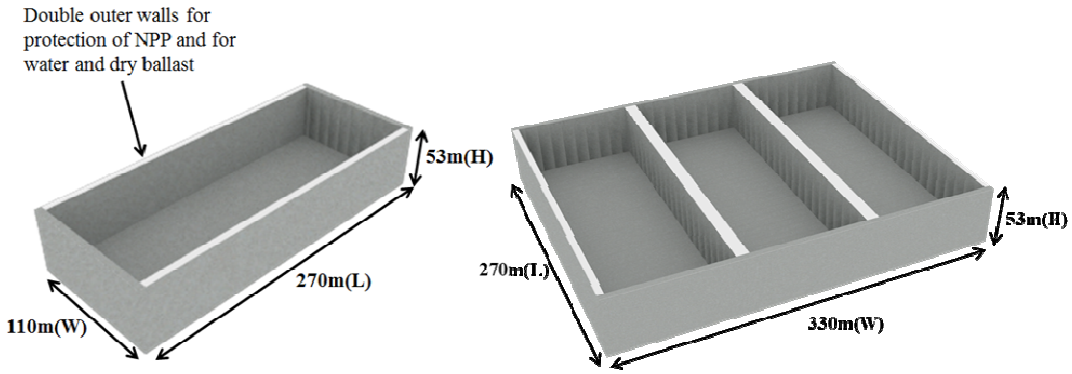

Fig. 8. Design dimensions of single and total GBS module

The APR1400 model is composed of two independent reactor units and turbine generator buildings. However, the compound building, intake structure building, and other site facilities are shared by the two reactor units and turbine generator buildings. The GBS type ONPP also has independent two reactor units and turbine generator buildings and shares the compound building, and control building. However, in contradistinction to the APR1400, the GBS type ONPP cannot share its site facilities, because each reactor unit and its related facilities are separated into GBS Module 1 and GBS Module 3; thus, the site facilities should be separated into GBS Module 1 and GBS Module 3 accordingly. In general, the site facilities of NPP are responsible for storing, monitoring, and supporting the NPP systems. In this study, most site facilities are assigned to Groups ①, ③, and ⑥. The GBS type ONPP is composed of three GBS modules: GBS Modules 1 and 3 contain Groups ①, ②, ③, ④, ⑥, and ⑦, but the vertical and horizontal arrangement direction of GBS Module 3 are opposite to that of GBS Module 1 to prevent differential settlement due to the symmetric structure arrangement.

GBS Module 2 is composed of two Group ⑧ sections and a single Group ⑤ section. The two intake structures and facilities are positioned in GBS Module 2 to supply cooling water to GBS Modules 1 and 3. The main control building and compound buildings are placed in the center of the GBS type ONPP for convenience of maintaining and controlling the entire system. The accommodation and refuges for workers must be located above the compound building because if flooding occurs, these places must be located above the maximum flooding water level. The assembly process of GBS Modules 1, 2, and 3 are shown in Figures 9 and 10, and the side view of each GBS module and its component groups are shown as Figures 11 and 12. The final concept design of the proposed GBS type ONPP is shown in Figures 13 and 14.

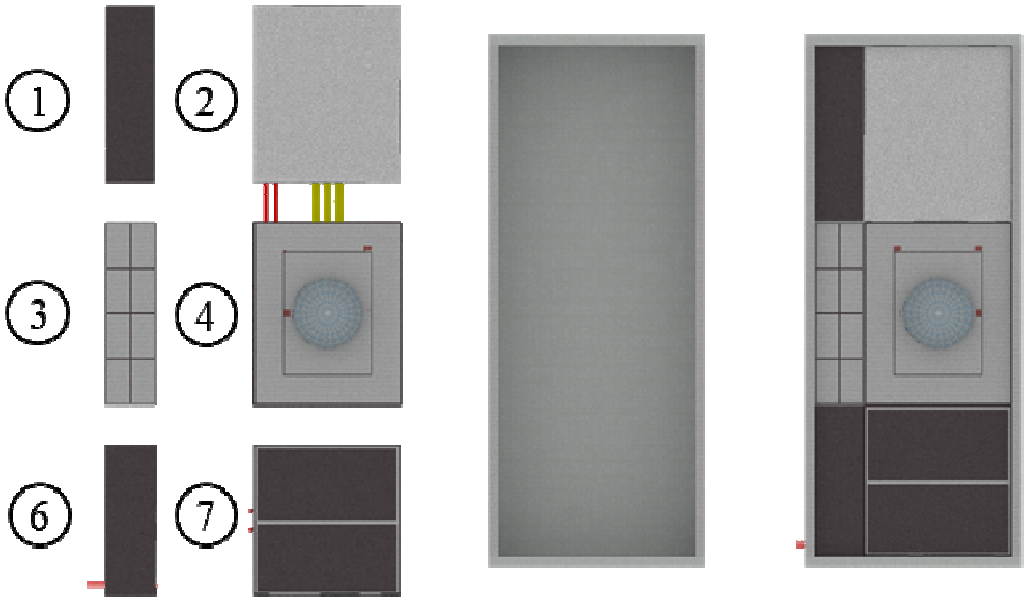

Fig. 9. Assembly of the element groups and GBS Modules 1 and 3

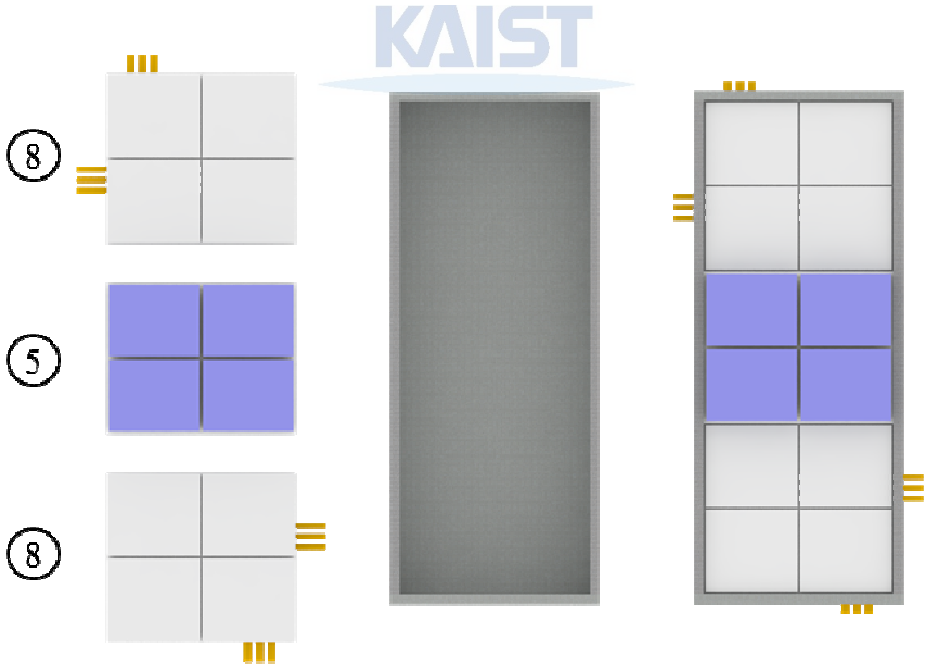

Fig. 10. Assembly of element groups and GBS Module 2

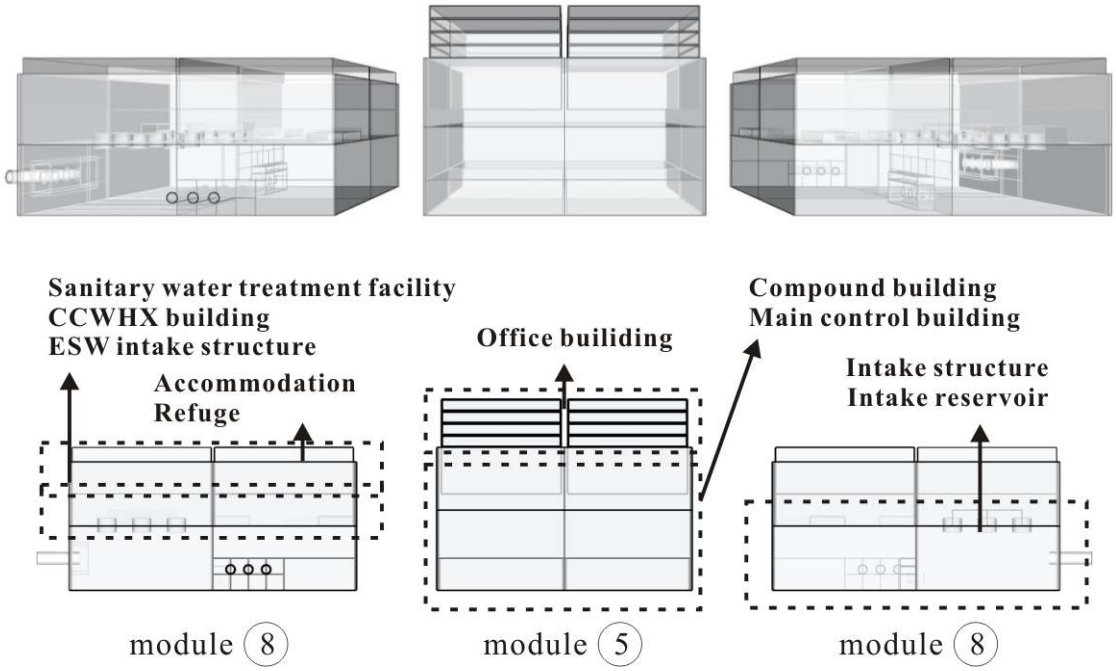

Fig. 11. Side view of GBS Module 2: group ⑧ and group ⑤ are the components of GBS Module 2

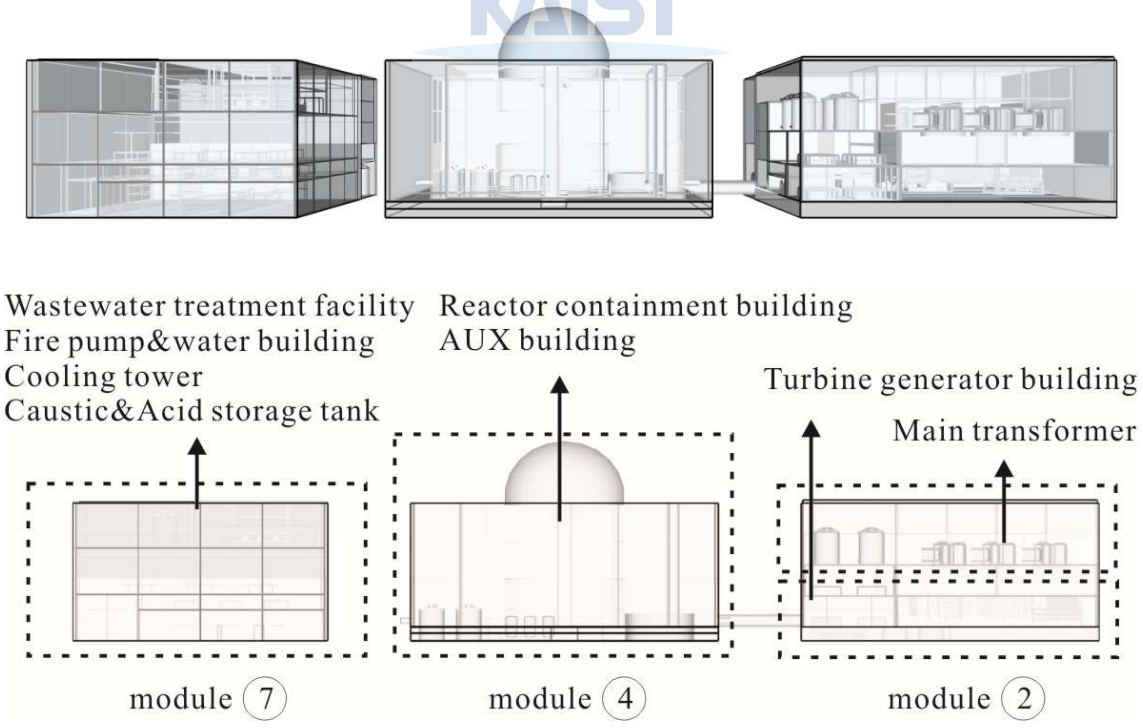

Fig. 12. Figure 12. Side view of GBS Modules 1 and 3: group ⑦, group ④, and group ② are the components of GBS Modules 1 and 3

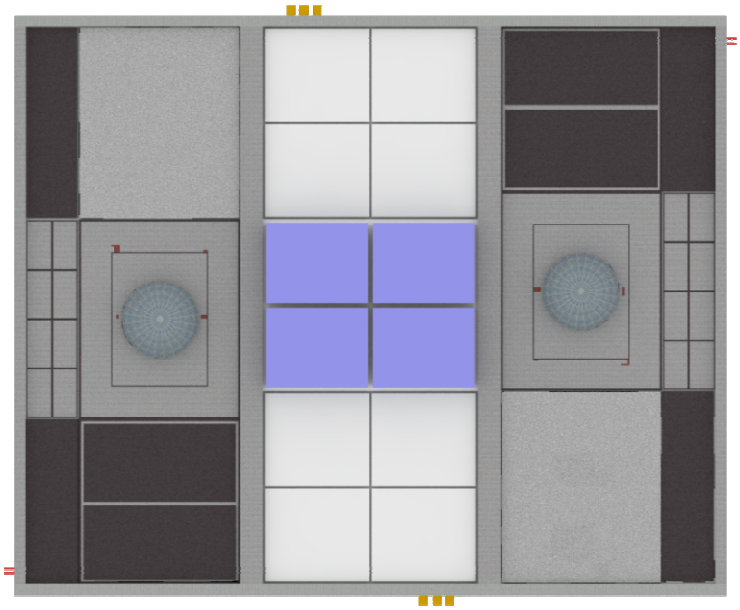

Fig. 13. Floor plan of the GBS type ONPP

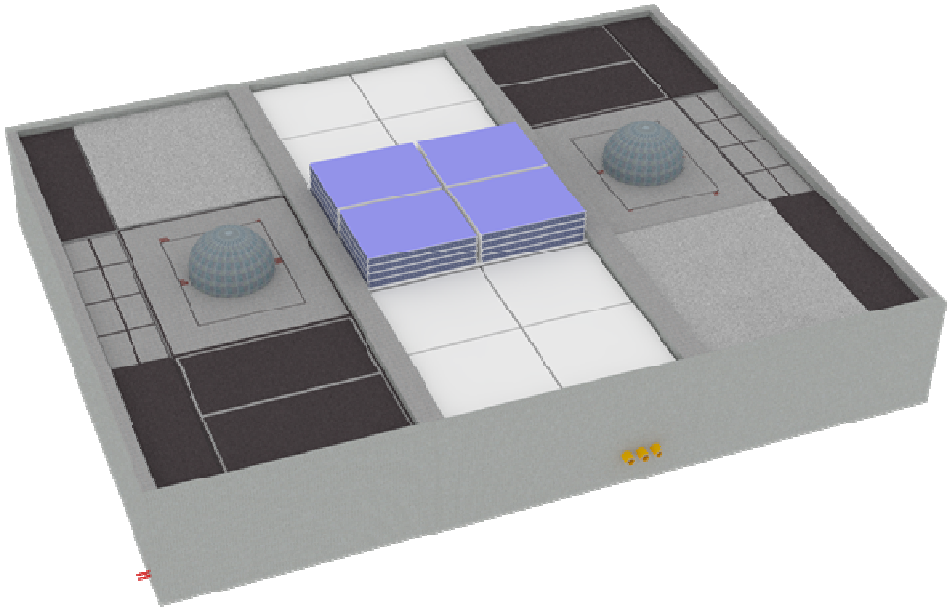

Fig. 14. Top view of the GBS type ONPP

Chapter 3. Safety Features of the GBS type ONPP

In the past three decades, the typical nuclear accident cases are the Fukushima Daiichi nuclear disaster (2011, Japan), Chernobyl accident (1986, Ukraine (FSU)) and the Three Mile Island (TMI) nuclear accident (1979, United States). In the Fukushima case, the nuclear disaster resulted primarily from the earthquake, which collapsed a transmission tower. With the loss of the off-site power, the emergency power system worked normally, but when the tsunami that resulted from the earthquake struck the NPP, the emergency diesel generator (EDG) were submerged and component cooling system, seawater pump, and fuel tanks were destroyed. Finally, the ECCS and circulating cooling system were suspended due to the NPP losing power. In case of TMI accident, the accident arose with failures in the non-nuclear secondary system, followed by a pilot-operated relief valve (PORV) being stuck open in the primary system, which allowed large amounts of the nuclear reactor coolant to escape. This caused a partial meltdown of the reactor core.

As demonstrated by these two nuclear accidents, the weak spot of the NPP is that the continuous supply of coolant without electrical power is impossible in the event of a major accident and they are easily affected by natural disasters such as earthquakes and tsunamis. The NPPs in the future should be immune to any kinds of expected natural disasters combined with loss of active power supply by providing adequate cooling under a given condition.

Unlike NPPs, ONPPs have ample cooling water because they are surrounded by seawater, and in emergencies, seawater can be used as a backup for cooling when the existing active system is failed due to unforeseen reason. That is, the ONPP can have a coolant supplied passively from ocean into the reactor containment building using a natural differential head between the ocean and inside the reactor containment building for power outages. In this study, new emergency passive cooling systems (EPCS) are suggested that use seawater along with ballast water.

In addition to the securing of an ample source of cooling water, the GBS type ONPP has benefits against earthquakes, tsunamis, storms, and marine collisions. We describe the safety features of the GBS type ONPP used to overcome natural disaster and marine accidents are described in the following sections.

3.1 Emergency passive containment cooling system (EPCCS) & emergency passive reactor-vessel cooling system (EPRVCS)

APR1400 model has active cooling system such as the emergency core cooling system (ECCS), emergency diesel generator (EDG), containment spray system (CSS) and in-vessel retention (IVR) as shown in Figure 15. However, when there is a total station blackout, where both onsite and offsite power are lost, the above active cooling system cannot function properly, consequently resulting in an accident being propagated and becoming a disaster such as the Fukushima nuclear disasters. After the TMI nuclear accident in 1979, the EPCS was adopted internationally as a design improvement to increase the safety margin and reduce the investment risk. The driving forces of the passive system are natural phenomena such as pressure and gravity. Therefore, the system is relatively simple and the reliability of operational performance is high. In particular, after the Fukushima nuclear disaster, there is a growing desire for a passive core cooling system that can remove the residual heat for long term.

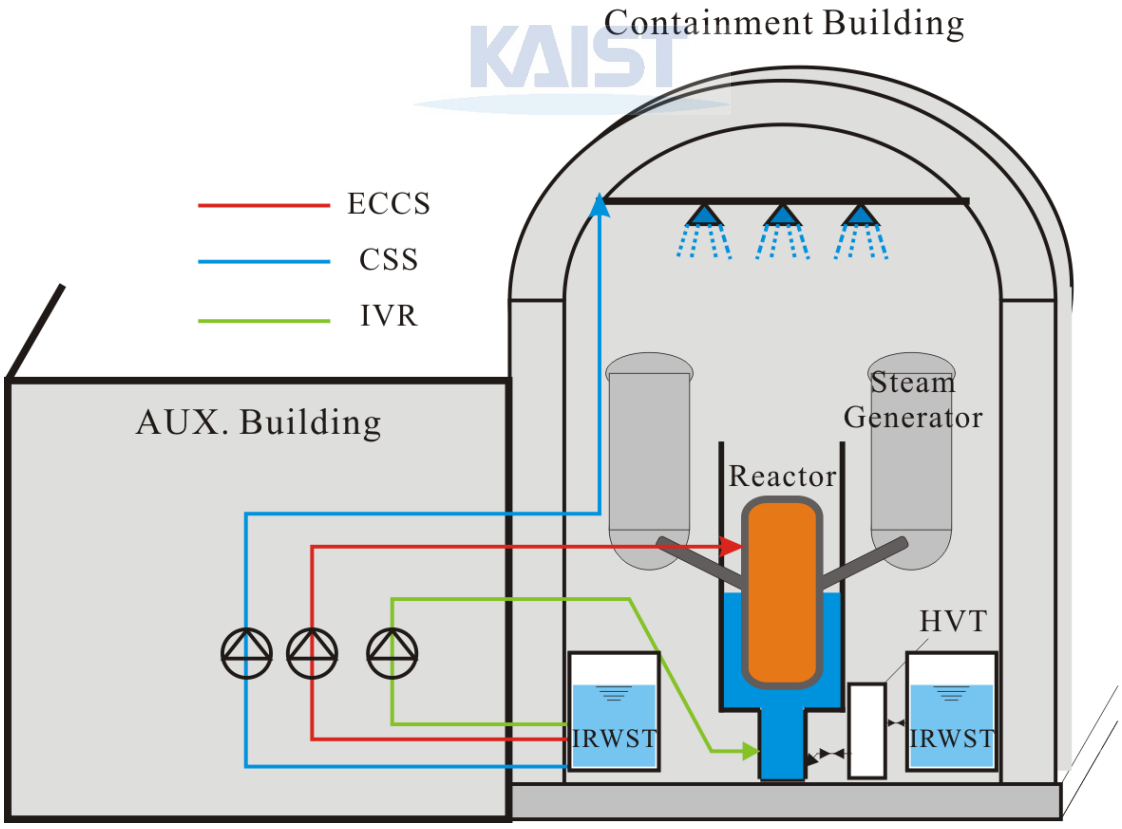

Fig. 15. Active cooling system of APR1400 model; emergency core cooling system (ECCS), containment spray pumps(CSS), and in-vessel retention (IVR)

A good example of nuclear reactor that has adopted a passive safety system is the AP1000 system designed by Westinghouse (USA). The AP1000 is a model that is 1000 MWe NPP, and the AP1000 has several passive safety features including a passive core cooling system and passive containment cooling system

Also, passive fluidic device is installed at the SIT for APR1400 to control the flsaw without any interventions, and another passive system (passive auxiliary feedwater system; PAFS) is now being developed for the APR+ model by Korea Hydro & Nuclear Power Co., Ltd. However, these passive systems are being developed for land-based NPPs. Thus, in this paper, addition to the established active and passive cooling systems, the EPCCS and EPRVCS are proposed as a passive cooling system for the GBS type ONPP; these passive cooling systems use the natural differential head between the ballast compartments and inside of containment as a driving force of the passive system.

3.1.1 EPCCS concept

During a certain type of accident scenario, pressure can be elevated gradually in the containment if the containment cooling system fails. For instance during a total station black out accident, reducing pressure inside the containment may not be possible with current APR1400 system design since it relies on the active containment cooling system. As a remedy to this situation, the ONPP can be equipped with a heat exchanger using ballast water as a coolant and operating by natural differential head due to steam generation inside the heat exchanger and the water level in the ballast water compartment. The detailed concept of the EPCCS is shown in Figure 16 (a) and the components of the systems are as follows:

- Steam delivery pipeline
- Ballast compartment and ballast water,
- Ballast water pipeline
- Heat exchanger
- Filtered venting system

A GBS has a ballasting system, and the ballasting compartment is filled with water or solid material (e.g. sand); if necessary, both materials are used. The ballasting tank acts as a condenser and cold water source in case when the active containment cooling system is not available. As shown in Figure 16(a), a heat exchanger is installed in

containment. The cold water source is supplied from the ballast water compartment. During an accident, steam is generated within the heat exchanger due to elevated temperature in the containment and the generated steam is delivered to the ballasting compartments by steam delivery pipeline. In this system, ballasting compartment is acting as a condenser. The ballast water constantly circulates the system to cool down the containment and reduce the pressure inside it to prevent from containment failing. However, the amount of ballast water might be insufficient to continuously supply cold water until the containment is sufficiently cooled. Hence, in the design phase, in order to secure sufficient ballast water for coolant, the size of the ballasting cell must be designed to be larger than the other ballasting cells. Furthermore, the ballasting cell is connected to sea via passive valve so that when the pressure and temperature of ballasting cell are too high, in can be relieved through this safety relief valve.

To cool the containment more efficiently and evenly, multiple heat exchangers installation is suggested in this paper and depicted in Figure 17 (b). EPCCS can be consisted of multiple heat exchangers connected to several ballasting compartments because GBS is surrounded by several ballasting compartments. However, generated steam from a heat exchanger can obtain radioactive matter even though the heat exchanger physically separates containment steam-air mixture from ballast water. Therefore filtered venting system is required on the steam delivery pipeline to reduce the risk of uncontrolled radiation release to the environment. The system is commonly consisted of scrubbing chamber and metal filter.

The purpose of the EPCCS is to cool and decrease the inner pressure of the containment. However, EPCCS can sufficiently cool the containment but in cannot prevent the reactor vessel failure if the accident proceeds to the beyond design accident when the core is severely damaged like TMI or Fukushima. In the following chapter, in order to protect the reactor vessel form failing during a severe accident, an emergency passive reactor-vessel cooling system (EPRVCS) is proposed; it is a system that directly cools the reactor-vessel using ballast water/seawater.

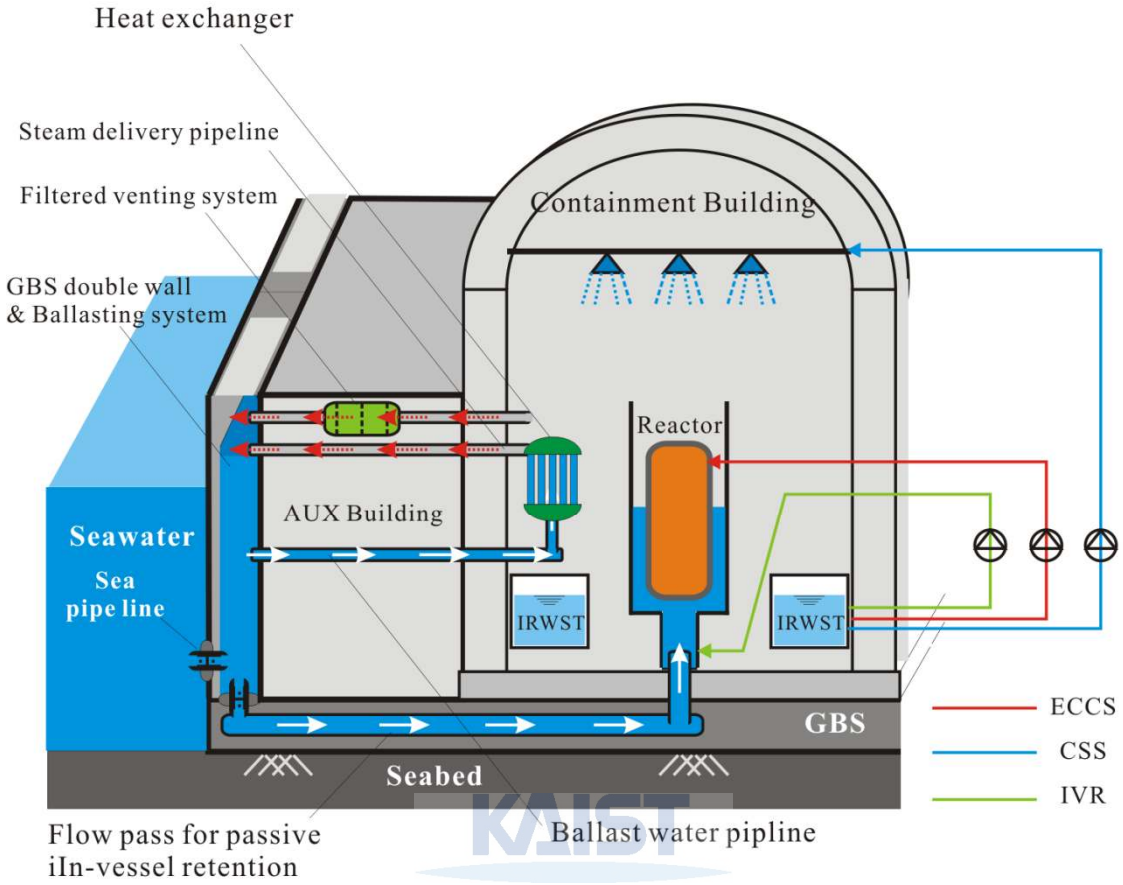

(a)

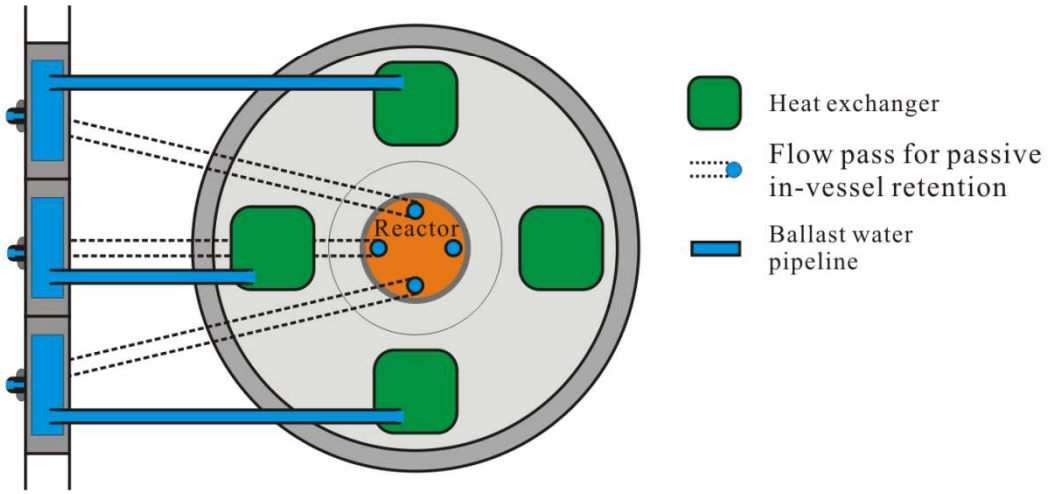

(b)

Fig. 16. Concept design of the emergency containment cooling system (EPCCS) and emergency passive reactor-vessel cooling system (EPRVCS)

3.1.2 EPRVCS concept

In contradistinction to the EPCCS, the EPRVCS cools the reactor vessel directly using ballast water/seawater if the accident results in severe core damage. In other words, this is a passive in vessel retention (IVR) strategy which utilizes the full potential of ONPP. In this case, addition to the EPCCS, passing through the flow pass for passive in-vessel retention, the ballast water is sent directly to the reactor vessel wall and fills up the reactor cavity to externally protect the reactor vessel from relocated nuclear fuel. The components of the EPRVCS are as follows:

- Filtered venting system
- Ballasting compartment and ballast water,
- Flow path for passive in-vessel retention
- Sea pipeline.

If the melting or significant degradation of the reactor core is expected or confirmed based on the information available and the adequate core cooling is not expected, the cooling and confinement of the core melt in vessel through external vessel cooling can be pursued. If the pressure in the containment is higher than the hydraulic head, the containment pressure can be balanced by EPCCS. After securing adequate hydraulic head, the pressure valve attached at the end of the passive in-vessel retention line is open and the ballast cells' water continuously flow into the reactor cavity and directly cools the reactor vessel by using the natural differential head between ballast compartments and inside of containment. When the water and reactor vessel come into contact, steam is generated in the containment. In this phase, containment is cooled by EPCCS as heat sink and condensed steam is stored in the IRWST as shown in Figure 16(a).

The EPRVCS uses ballast water to flood the reactor vessel up to hot legs and cold legs. The produced steam from the boiling on the reactor vessel surface can be condensed by EPCCS and return to the reactor cavity by gravity. The long-term cooling of reactor vessel can be maintained by this natural recirculation of water. By the cooling and confinement of core melt in vessel, a severe accident can be terminated in vessel and thus the release of fission products to the containment can also be minimized. By protecting the reactor and containment using EPRVCS and EPCCS respectively, any significant offsite radiological consequence can be prevented as we experienced in TMI-

2 accident.

3.2 Seismic effect

Adding to the GBS's weight, the ballasting compartment is filled with water or a solid material to secure sufficient gravity. That is, the total weight of the GBS is changeable and can be controlled using the ballasting and deballasting systems. Under the seismic loading, the weight of the structure is a dominant factor of the dynamic response of the structure. By reducing the total weight of the GBS, an effective seismic isolation effect can be expected. The seismic isolation technologies have already been applied to land-based nuclear power plants and other plants in several countries.

The principle of the base isolation system is the decoupling of a superstructure from its substructure. There are many isolation devices, for example steel and rubber bearings, energy absorbers, hydraulic devices, and friction systems. This paper focuses on the friction system. The friction system is governed by the friction force between the superstructure and substructure. The friction force is the function of the coefficient of friction and total weight of the superstructure. The coefficient of friction is a dimensionless scalar value that describes the ratio of the force of the friction between two bodies and it depends on the materials used. That is, the friction coefficient of concrete versus soil cannot be changed, but the total weight of GBS type ONPP can be controlled.

There are two methods to change the total weight of the GBS. The first method is using the ballasting system. By discharging the contained ballast water in the ballasting compartments, the GBS total weight can be reduced. The second method is attaching a large buoy to the structure; this method is already used for to control the GBS balance in offshore oil platforms. In short, by reducing the total weight of GBS, the vertical load acting on the seabed can be reduced, and then the friction force at the GBS bottom is reduced. Consequently, the GBS slides more easily in which state it acts as friction base isolation system. The details of the principle of the base isolation mechanism and GBS friction base isolation system are explained and shown in Figure 17.

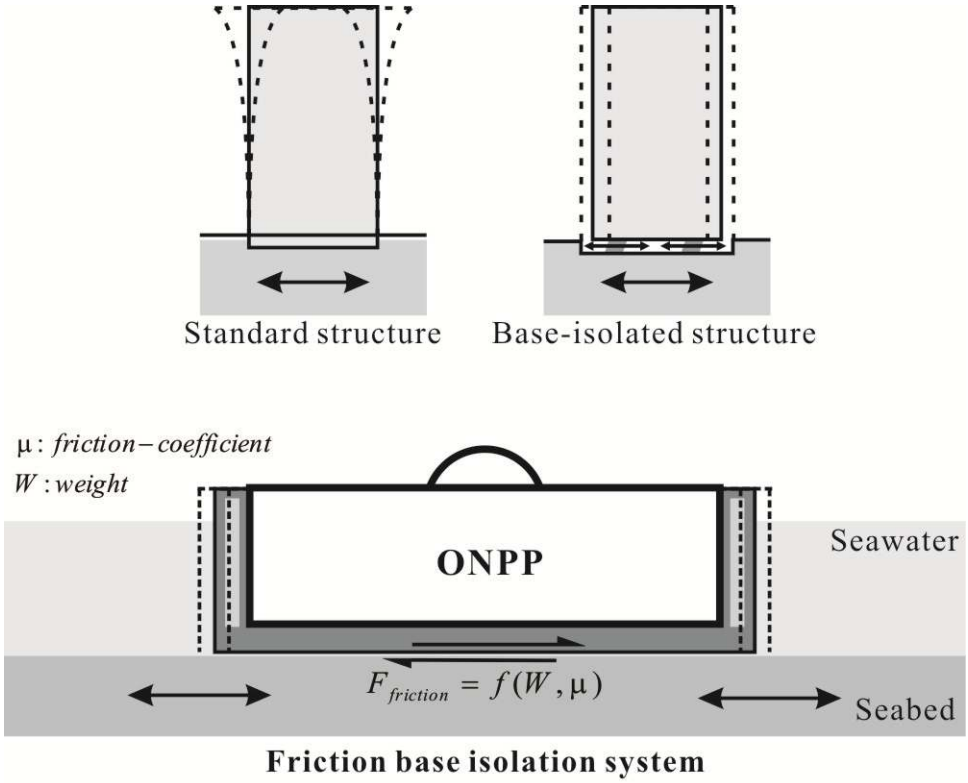

Fig. 17. Mechanism of the base-isolation system and GBS friction base isolation system governed by friction coefficient (μ) and weight (W)

Although the failure mode of a GBS is a sliding condition, during an earthquake, the safety of the GBS type ONPP can be increased. In a normal state, in order to prevent the sliding of the GBS modules due to severe wave loads or other external ocean environmental loads, sufficient shear resistance at the base is provided by a corrugated steel skirt driven into the ground. For the Adriatic LNG Terminal, a 1 m corrugated steel skirt is extended into the ground, but the skirts below the base slab are usually designed to yield during an extreme earthquake. Furthermore, in addition to the base isolation effects, the kinematic energy of the structures caused by the earthquake can be absorbed by the surrounding seawater, which acts as a natural damper.

In order to clarify the effects of the base isolation and seawater damping, a dynamic response analysis of GBS during a real earthquake is essential, which includes research into the fluid-structure-soil interactions and remains for future study.

3.3 Safety against tsunamis and marine collisions

Due to the ease of securing the circulating cooling water and the problem of public acceptance, land-based NPPs have mostly been located near the seaside but far from residential areas. Thus, in the event of a natural disaster such as a tsunami, land-based NPPs are easily damaged as in the Fukushima nuclear disaster.

The main cause of the Fukushima nuclear accident was a power outage due to the tsunami inundating the EDG facilities. Tsunamis have a small amplitude and a very long wavelength in the open sea, which allows them to pass unnoticed at sea, forming only a slight swell usually about 300 millimeters above the normal sea surface. However, the tsunami wave height increases rapidly to tens of meters when they reach shallow water on the coastline. By using a shallow water equation and energy flux conservation theorem, the tsunami height can be estimated at a certain water depth. When it is considered that the tsunami is a long wave, the shallow water equation can be written simply in terms of water depth, as follows:

$$C = \sqrt{gh}, \tag{1}$$

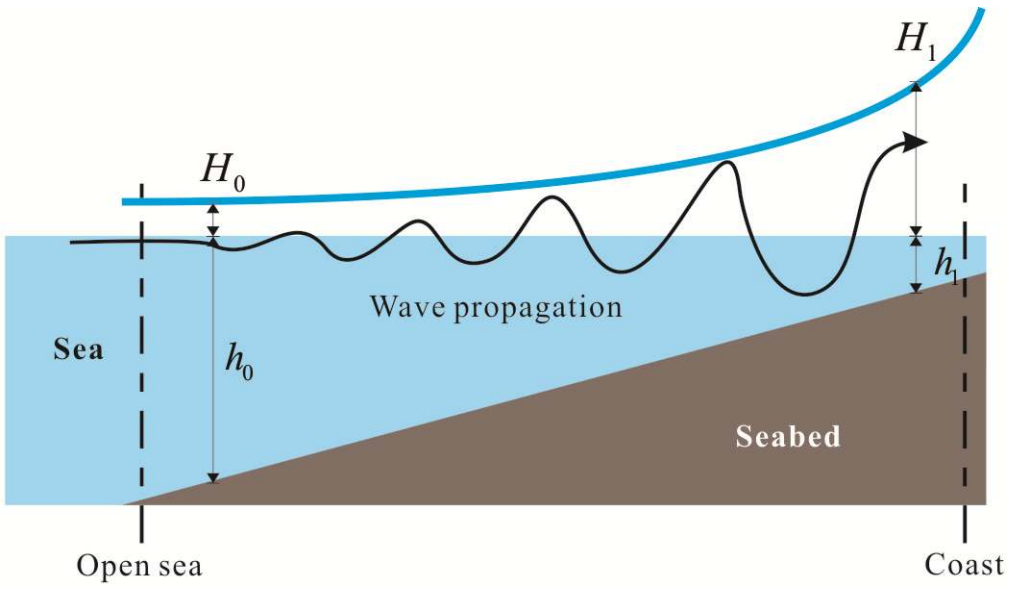

Fig. 18. Tsunami wave height increases as it moves closer to the shoreline

where C is the wave velocity, and g and h are the gravity acceleration and water depth, respectively. As shown in Figure 18, based on the energy flux conservation theorem, the total energy in the open sea is the same as the total energy at the coastline. The energy flux conservation equation is as follows:

$$(\mathrm{E}C_0)_0 = (\mathrm{E}C_1)_1 \tag{2}$$

and when equation (1) is substituted into equation (2), the tsunami height formula can be obtained in terms of water depth:

$$H_0 = H_1\left(\frac{h_1}{h_0}\right)^{1/4} \tag{3}$$

where the subscripts 0 and 1 indicate the position of the open sea and coastline, respectively, and H and h are the tsunami height and water depth, respectively. In order to obtain the tsunami height from this equation, the proper value of h_1 must be set. When h_1 is close to zero, the tsunami height at the coastline does not converge. The reason is that equation (3) does not reflect the effect of the wave breaking, so the tsunami height multiplies toward infinity.

According to the GPS wave height meter that was placed in the waters 20 kilometers off Fukushima and at a depth of 204 meters, the observed maximum tsunami height was 6.7 meters. Based on the observed tsunami height data, the tsunami height at the target ONPP's water depth 30 meters can be calculated using equation (4):

$$H_0 = H_{ONPP}\left(\frac{h_{ONPP}}{h_0}\right)^{1/4} \tag{4}$$

where $H_0 = 6.7$ m, $h_0 = 204$ m and $h_{ONPP} = 30$ m. Consequently, the calculated tsunami height at the ONPP is 12 meters. The designed total height of the GBS type ONPP is 53 meters, so approximately 11 meters of freeboard can be secured if a tsunami in the same class as that of Fukushima occurs. These calculated data demonstrate that the GBS type ONPP is relatively safer than land-based NPPs in the event of a tsunami. 11 meters of freeboard is sufficient to prevent the inundating of the safety systems and

facilities mounted on the GBS.

When an offshore structure is designed to counteract tsunamis, the marine collisions resulting from floating objects that accompany the propagating wave must also be considered. Indeed, many shore facilities have been destroyed by floating objects when tsunamis have occurred. The GBS concrete caisson is durable against impact load such as marine collisions because the GBS is surrounded by concrete double walls and a concrete bottom. Due to these two layers of walls, any loss to the GBS type ONPP's facilities and systems while accidents occur are significantly minimized. If one layer is damaged due to a collision or similar accident, the second layer acts as a back up and prevents the ingress of seawater into the GBS.

Chapter 4. Modeling procedure for dynamic response analysis of GBS

4.1 GBS modeling

As a preliminary study, authors have been developed concept design of GBS type Ocean Nuclear Power Plant (ONPP). As mentioned before, land based nuclear power plant APR1400 is mounted on the GBS and another concept model is also suggested which based on the SMART. The target concept model for the dynamic analysis of this study is SMART based GBS type ONPP. The overall dimension of SMART based GBS type ONPP is shown in Figure 19. In finite element (FE) model, the GBS is modeled using nine node elements with plane strain formulation, as the longitudinal and horizontal dimensions are same as 168 m, respectively and using a linear isotropic material.

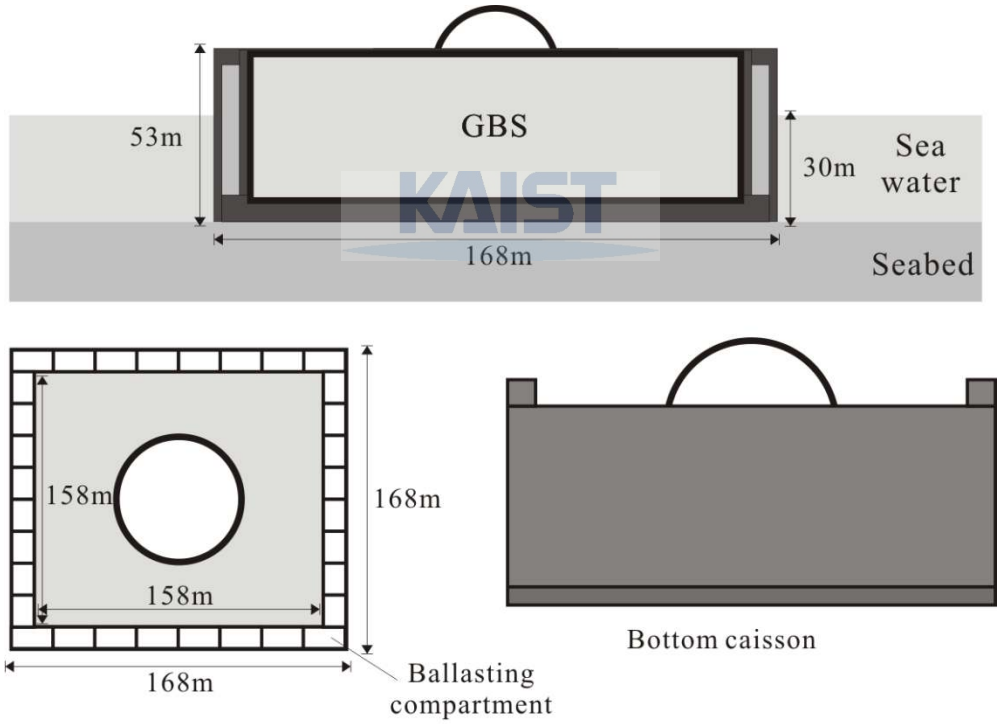

Fig. 19. Overall dimension of GBS type ONPP based on SMART

4.2 Fluid-structure interaction

There has been considerable amount of researches conducted to study seismic response with fluid-structure interaction of quay wall and dam-reservoir system. Quay wall and dam-reservoir systems are kinds of fluid-structure interaction problems. During

earthquake hydrodynamic forces are applying to the vertical wall due to motion of quay wall and at the same moment compression waves are generated and transmitted through the fluid. During last 50 years, research dealing with the dam-reservoir systems has been conducted to understand dynamic behavior. The first thorough analysis of hydrodynamic forces on vertical walls during earthquake was reported by Westergaard [1] in 1933. Westergaard`s analytical solution assumed that the dam behaves rigid body and the water is incompressible, but the results has been widely used for research of dam-reservoir system during earthquake. GBS is also surrounded by seawater, therefore hydrodynamic forces are acting on the vertical wall of GBS during earthquake and dynamic response of GBS is affected by hydrodynamic forces. To investigate the dynamic behavior of GBS during earthquake, FSI effects have to be considered in the analysis.

The main equations direct symmetric coupled formulation based on $\phi - U$ potential-based formulation developed by Bathe and Oslon [2] has been implemented in ADINA-finite element software. Velocity potential (ϕ) is used as the nodal variables in the fluid domain, and the displacement (U) indicates the nodal variable in the solid. A coupling matrix (C) couples the fluid to the solid, and links the pressure to the velocity potential in a fluid domain. In the fluid, assuming an irrotational water motion with no heat transfer, inviscid, infinitesimal velocity and density change, relatively small displacements of the fluid and no actual fluid flow implies the existence of a velocity potential satisfying the equation of continuity and energy conservation as written by:

$$\nabla\phi = \mathbf{v}; \quad \dot{\rho} + \nabla\cdot(\rho\nabla\phi) = 0; \quad \frac{\partial\phi}{\partial t} = -\frac{p}{\rho} \tag{5}$$

where ∇ is the vector gradient, $\mathbf{v}$ is the velocity vector of fluid particle, ρ is the water density, ϕ is the velocity potential. Using the classical Galerkin discretization technique, the coupled to the equation of motion of the structure which yield to;

$$\begin{bmatrix} M_{SS} & 0 \\ 0 & -M_{FF} \end{bmatrix}\begin{bmatrix} \ddot{U} \\ \ddot{\phi} \end{bmatrix} + \begin{bmatrix} C_{SS} & C_{FS}^{T} \\ C_{FS} & C_{FF} \end{bmatrix}\begin{bmatrix} \dot{U} \\ \dot{\phi} \end{bmatrix} + \begin{bmatrix} K_{SS} & 0 \\ 0 & -K_{FF} \end{bmatrix}\begin{bmatrix} U \\ \phi \end{bmatrix} = \begin{bmatrix} R \\ 0 \end{bmatrix} + \begin{bmatrix} (R_{SB})_S \\ 0 \end{bmatrix} + \begin{bmatrix} 0 \\ -\dot{R}_{FB} \end{bmatrix} \tag{6}$$

Where K_{SS} and M_{SS} represent stiffness and mass matrix for the solid elements and K_{FF} and M_{FF} those for fluid elements. FSI elements enforce coupling between the

fluid and solid region through the C_{FS} matrix. C_{SS} is Rayleigh damping matrix and C_{FF} account for damping due to energy dissipation at the fluid domain boundary. FSI interface elements are imposed on the interface of seawater and GBS vertical wall as well as in the interface of seawater and seabed line. Each node of the element contains the potential degree of freedom and displacement degrees of freedom. It is assumed that the displacements of the nodes of the interface element are small. The transient solution of a fluid-structure interaction problem is solved by numerically integrating by equation with implicit New-mark time integration schemes. In this study nine node potential-based fluid elements are used for seawater.

To model the boundary interfaces of fluid domain, in this study, free surface boundary and infinite boundary are used. To model the free surface of seawater, “Free surface interface element” is used which provide for the boundary of a potential-based fluid element, in ADINA.

When we analyze such dam-reservoir system, quay wall or offshore structure under earthquake, modeling a sufficiently large domain of fluid becomes too expensive for extended time analyses. To overcome these difficulties many alternative approaches has been invented. In 1985, Oslon and Bathe suggested an infinite element based on the doubly asymptotic approximation (DAA) method for use in finite element analysis of FSI problem. In DAA technique, the plane wave is approximated at high frequencies and the added mass is approximated at low frequencies. Oslon and Bathe choose to apply the DAA as infinite elements which model the fluid far from the structure, while suing finite elements near the solid. This method is implemented in ADINA and we will use the “infinite interface elements” for the infinite boundary condition to account for the effects of the outer fluid on the inner region.

4.3 Soil-structure interaction

The primary concern of dynamic soil-structure interaction (SSI) effects and their effects on structural dynamic response under various earthquake and site soil condition are the difficulties of SSI problems. The analysis is commonly conducted in the frequency domain, but for the more realistic simulation, nonlinear effects must be considered in time domain [3]; where the basic equation of motion is formulated to analyze the interaction of a non-linear structure and an irregular soil with the linear unbounded soil in time domain.

In this study, for modeling of non-linear behavior and failure of soil model, the Mohr-Coulomb model is used. The Mohr-Coulomb model is based on; a non-associated flow rule, a perfectly-plastic yield behavior and tension cut-off [4]. However, Mohr-Coulomb model has tendency to overestimate plastic volume strain than observed in the real soil. Also, beyond yield criteria soil permanently dilate. Although, Mohr-Coulomb model has unrealistic and shows unreasonable results in some problem, it is widely used for modeling of non-linear soil dynamic behavior due to its simplicity and also accuracy is acceptable enough. The Mohr-Coulomb yield equation can be written as

$$f_{MC} = \alpha I_1 + \sqrt{J_2} - k \tag{7}$$

where α and k are stress dependent

$$\alpha = \frac{2\sin\phi}{3(1-\sin\phi)\sin\theta + \sqrt{3}(3+\sin\phi)\cos\theta}$$

$$k = \frac{6C\cos\phi}{3(1-\sin\phi)\sin\theta + \sqrt{3}(3+\sin\phi)\cos\theta} \tag{8}$$

where ϕ indicates friction angle, C is the cohesion, I_1 is the first stress invariant and J_2 is second deviatoric stress invariant. In here, we note that hardening rules does not apply to the Mohr-Coulomb model; the Mohr-Coulomb model is only used in conjunction with the elastic-perfectly-plastic yield condition [4].

Under the earthquake, progressive wave are generated in the soil domain in horizontal and vertical direction respectively. Unfortunately, these progressive waves are reflected and superimposed due to usual finite boundary of the finite element model. A simple solution to eliminate such phenomenon is to move the finite boundary far away from the structure so the dynamic behavior of structure does not affected by boundary effects. However, this method is too expensive for time analyses. Therefore, to simulate a boundary condition that ensures that all energy arriving at the boundary is absorbed, the viscous damping boundary is modeled at the end side of soil domain boundary. Using the method proposed by Lysmer and Kuhlemeyer in 1969 [5], the absorptive condition at the end of soil domain can be modeled by a series of viscous dampers placed at the

end of soil domain. The technique of Lysmer and Kuhlemeyer`s, boundary condition is expressed by the following equations.

$$\sigma = a\rho V_P \dot{w}$$

$$\tau = b\rho V_S \dot{u} \tag{9}$$

These equations are depend on the normal and tangential velocities $\dot{w}$ and $\dot{u}$. In the above equations, ρ , V_P, and V_S denote the local values of the material density, longitudinal and shear wave velocities, respectively. a and b are dimensionless parameters. The longitudinal and shear wave velocities are calculated as

$$V_P = \sqrt{\frac{(1-\upsilon)E}{(1-2\upsilon)(1+\upsilon)\rho}} \tag{10}$$

$$V_S = \sqrt{\frac{E}{2(1+\upsilon)\rho}} \tag{11}$$

The modeling procedure of viscous damping boundary is simply conducted by ADINA. In the SSI analysis, soil and structure interface modeling is also important. In GBS bottom-soil interaction system, the relative motion of GBS under the earthquake is occurred against seabed motion. In the interface between GBS and seabed, factors such as interface roughness, state of stress, type and rate o f loading and modes of deformation influence on the dynamic behavior of GBS. Under the severe ground motion, relative motion such as sliding, slip or separation can be occurred at the interface. In [6], B. Haggblad and G. Nordgern demonstrated four basic modes of deformation at the soil-structure interface, which modes change the transferred forces to the structure: (1) stick or no-slip; (2) slip or sliding; (3) separation or debonding; and (4) rebonding. When the bottom of GBS is not bonded to the seabed, GBS can be in sliding or slip phase in horizontal direction during earthquake. To model such slip or sliding motion of GBS, contact condition is imposed to the GBS bottom and seabed interface in FE model. The sliding motion is governed by ideal Coulomb friction in present analysis so proper contact condition have to be defined before FE modeling. To fulfill the all contact condition at the contactor surface, the constraint-function method is selected.

The contact element which provided by ADINA are able to model either slippage or separation during static and dynamic analysis. The motion of the GBS relative to the ground is resisted by frictional force between the bottom of GBS and the ground surface. Selection of an appropriate value for the coefficient of friction μ is important. In this study, we select 0.4 as a default value for coefficient of friction. In the chapter 3.2.2, we will discuss more about the selection of coefficient of friction. The limiting value of the Coulomb friction force, F_S to which the sliding support with GBS can be expressed as:

$$F_S = \mu mg \tag{12}$$

where m is the mass of GBS and g is the acceleration due to gravity. In ADINA, for friction, a nondimensional friction variable τ can be defined as [4]:

$$\tau = \frac{F_S}{\mu mg} \tag{13}$$

The standard Coulomb friction condition can be expressed as:

$|\tau| \le 1$

and $|\tau| < 1$ implies $\dot{u} = 0$

while $|\tau| = 1$ implies $\text{sign}(\dot{u}) = \text{sign}(\tau)$

where $\dot{u}$ is the sliding velocity. This algorithm means that when τ is bigger than one, the GBS is in sliding condition.

Chapter 5. Dynamic analyses of GBS-seawater-soil system

5.1 GBS-seawater-soil interaction analysis

To verify the correct utilization of the FSI finite element modeling in ADINA, Arablouei et al [7], solved dam-reservoir system and they compared obtained results with the staggered solution scheme developed by Ghaemian and Ghobarah [8]. The presented

comparing results by Arablouei shows that the results of ADINA and staggered solution of Ghaemian and Ghobarah are a good agreement for both crest displacement and hydrodynamic pressure near the bottom of reservoir. Therefore, we can model the GBS-seawater-soil interaction system using FSI interface element which provided in ADNINA.

Addition to the fluid-structure interaction consideration, for the modeling of soil-structure interaction, Mohr-coulomb model are used in soil modeling and ideal Coulomb friction assumption is imposed at the interface between GBS bottom and seabed to model pure-friction behavior, which motions are investigated before intensively especially for the dam-reservoir systems [9, 10]. Under the severe ground motion, the dynamic behavior of GBS is similar like motion of concrete gravity dams. Hence, we imposed ideal Coulomb friction to model pure friction at the soil-structure interface.

5.1.1 FE model and material parameters for GBS-seawater-soil system

The design height of GBS is 53 meters and water depth is 30 meters for the analysis; the dimensions are originated from the concept design of GBS type ONPP. The truncated boundary distance from the GBS wall is 300 meters which values are ten times of submerged height of GBS(submerged height = 30 m) in order to reduce the boundary effects enough. The effects of truncated boundary distance are conducted by Arablouei et al [7]. From their research, we can realize that ten times of submerged depth of structure is enough for the boundary distance to eliminate reflection effects at the truncated boundaries. The detail FE model of GBS-seawater-soil system is shown in Figure 20. Where symbols of imposed boundaries are indicated as:

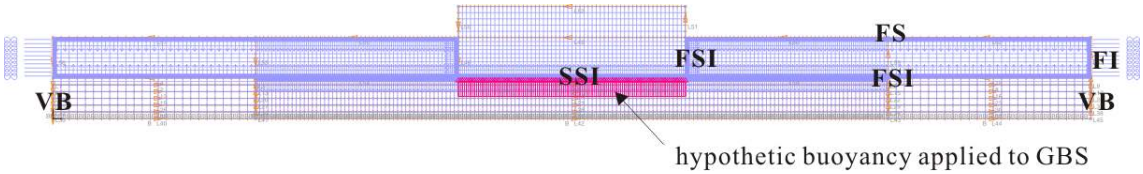

Fig. 20. FE model of GBS-seawater-soil system

FS : free surface boundary condition, ocean water surface

FI : fluid infinite boundary condition; ocean water truncated boundary

VB : viscous boundary condition; soil truncated boundary

FSI : fluid-structure interaction boundary condition; interface between GBS, soil and water

SSI : soil-structure interaction boundary condition; friction condition

The parameters for GBS, seawater and soil are presented in the Table 4, 5, 6 and 7, respectively. To model the seabed layer, Nevada sand at 75% relative density (*Dr*) is used. The parameters of the soil are selected based on the VELACS project data [11, 12]. Here, we note that the specific seabed information or condition for the GBS type ONPP are not yet decided so we choose above soil condition from Ref. [7] which research analyze Quay wall-soil-seawater system. For the seawater, bulk modulus and density is selected as 2.07×10^6 kPa and 1000 kg/m^3.

Table. 4. Parameters for reinforced concrete GBS

Parameters	Density(kg/m^3)	Young`s modulus(kpa)	Poisson`s ratio
GBS	2500	3E7	0.2

Table. 5. Parameters for seawater

Parameters	Density(kg/m^3)	Bulk modulus (kpa)
Sea water	1000	2.07E6

Table. 6. Parameters for soil

Parameters	Dry density(kg/m^3)	Internal friction angle(°)	Poisson`s ratio
Soil	1000	36	0.2

Table. 7. Young`s modulus and P-wave and S-wave velocity of soil layer (0~30m)

Soil layer	Depth(m)	E (Pa)	Vs(m/s)	Vp(m/s)
1	5	1.3E+08	173	507
2	10	2.24E+08	227	565
3	15	2.89E+08	258	602
4	20	3.41E+08	281	630
5	25	4.15E+08	310	668
6	30	4.29E+08	315	674

5.1.2 Input accelerations

For the GBS-seawater-soil system, four horizontal ground motions are selected. As an input ground motion three real earthquakes are selected, which are El-centro, Kobe and Tabas earthquake. Addition to the real earthquake, one artificial harmonic ground motion is used for the input acceleration. The characteristics of applied ground motion are show as Table 8 and the acceleration of time history duration time 15sec is show as Figure 21.

Table. 8. Characteristics of selected ground motion : Horizontal component

Earthquakes	Horizontal component	
	PGA (g)	Range of dominant frequencies
harmonic	0.3	2
El Centro - Imperial Valley	0.349	0.83-2.19
Kobe - Japan	0.599	0.97-2.50
Tabas – Iran	0.852	0.20-6.70

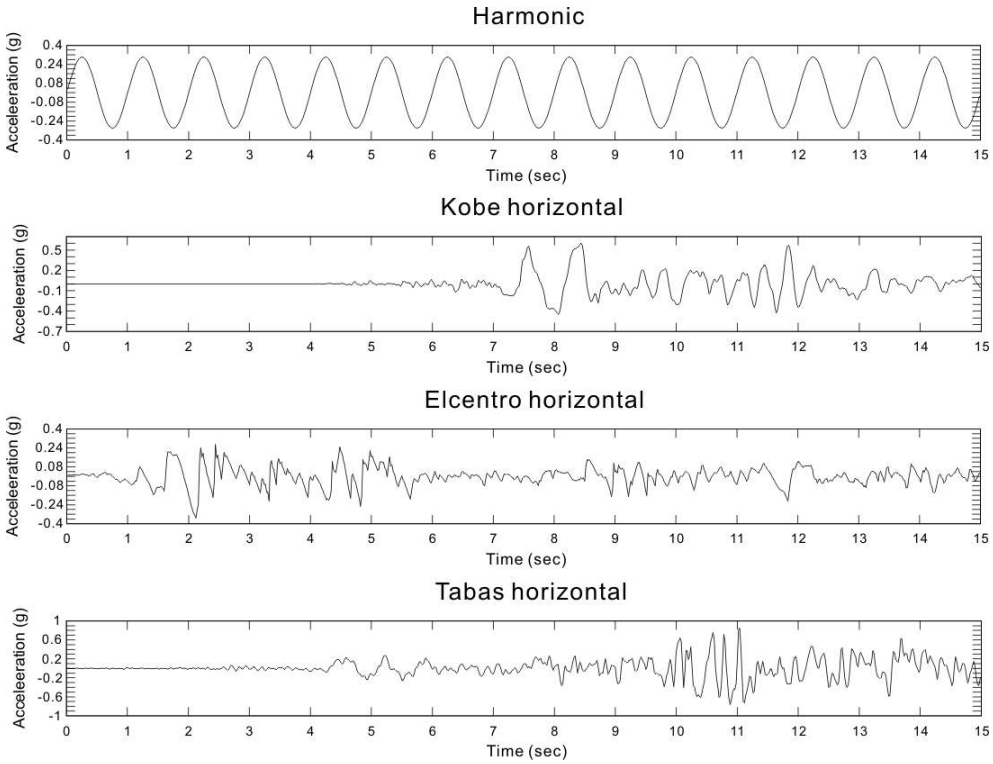

Fig. 21. Selected ground motion time history : duration time 15 sec

5.1.3 Floor response spectra

As mentioned before, Nuclear Power Plant (NPP) is mounted on the GBS. Damage on the operational and functional components of NPP is occurred during earthquakes. Operational and functional components include architectural components, mechanical and electrical equipment. A rational approach to designing these elements against seismic excitations involves the use of floor response spectra (FRS). Therefore, by using FRS, the dynamic floor response of GBS type ONPP can be analyzed. For the FRS approach, frequency domain is used from 0.5 to 25 Hz.

5.1.4 Dynamic analysis assumption

In this study, dynamic transient analysis is conducted. As mentioned before, for the contact analysis of GBS bottom and seabed interface, constraint function method is selected. The constraint function method is valid in dynamic-implicit solution method in ADINA contact algorithms [4], hence in this study dynamic-implicit integration solution method is used and for the integration parameters δ and α which used in Newmark method are taken as $\delta = 0.5$ and $\alpha = 0.25$, respectively. For the constraint function

method, suggested delta and alpha values are recommended in ADINA. The time step for the Newmark time integration is 0.02 second due to the selected real earthquake recorded with 0.02 second time step. Soil model is regarded as saturated condition

For the GBS and soil damping, Rayleigh damping which proportional to the mass and stiffness is used for generating damping matrix in ADINA and Rayleigh damping is expressed as:

$$\mathbf{C} = \alpha \mathbf{M} + \beta \mathbf{K} \tag{14}$$

where α and β are the coefficient of Rayleigh damping and through the coefficient, we can judge the importance of mass or stiffness for the structure damping system. To calculate the coefficient of Rayleigh damping, we need to conduct frequency analysis to obtain first two mode of GBS-seawater-soil system. The Rayleigh damping coefficient is calculated by following equation:

$$\alpha = \frac{2\omega_1\omega_2}{\omega_1 + \omega_2}\xi, \quad \beta = \frac{2}{\omega_1 + \omega_2}\xi \tag{15}$$

The ten fundamental frequencies of GBS-seawater-soil system are as shown in Table 9. The critical damping ratio of structure is represented by ξ. In this study, the damping ratio for GBS is taken as 5% and for soil model (e.g. Mohr-Coulomb) 2% is selected. In ADINA-system, α and β are assigned to the other element group separately.

Table. 9. The ten fundamental frequencies of GBS-seawater-soil system

Mode	GBS-seawater-soil system frequency (Hz)
f1	1.319
f2	2.202
f3	2.24
f4	2.331
f5	2.331
f6	2.569
f7	2.573
f8	2.829

f9	2.837
f10	3.171

5.2 Dynamic analysis for GBS-seawater-soil system

As mentioned before the target analysis model suggested in this study is GBS type Ocean Nuclear Power Plant (ONPP) which based on the SMART Nuclear Power Plant (NPP). The all specific dimension and analysis domain region are originated form the concept design of GBS type ONPP. Unlikely other dynamic response analysis of offshore structure under the earthquake, the presented problem in this study, nuclear power plant is mounted on the GBS so the response quantities of interest are the absolute maximum acceleration of the GBS at various stations. The important station to obtain acceleration response is shown as Figure 22. The suggested station at the GBS is related to the important facilities and systems for the NPP performance. The eighteen stations are selected to obtain acceleration responses and each station is aligned in around center of GBS.

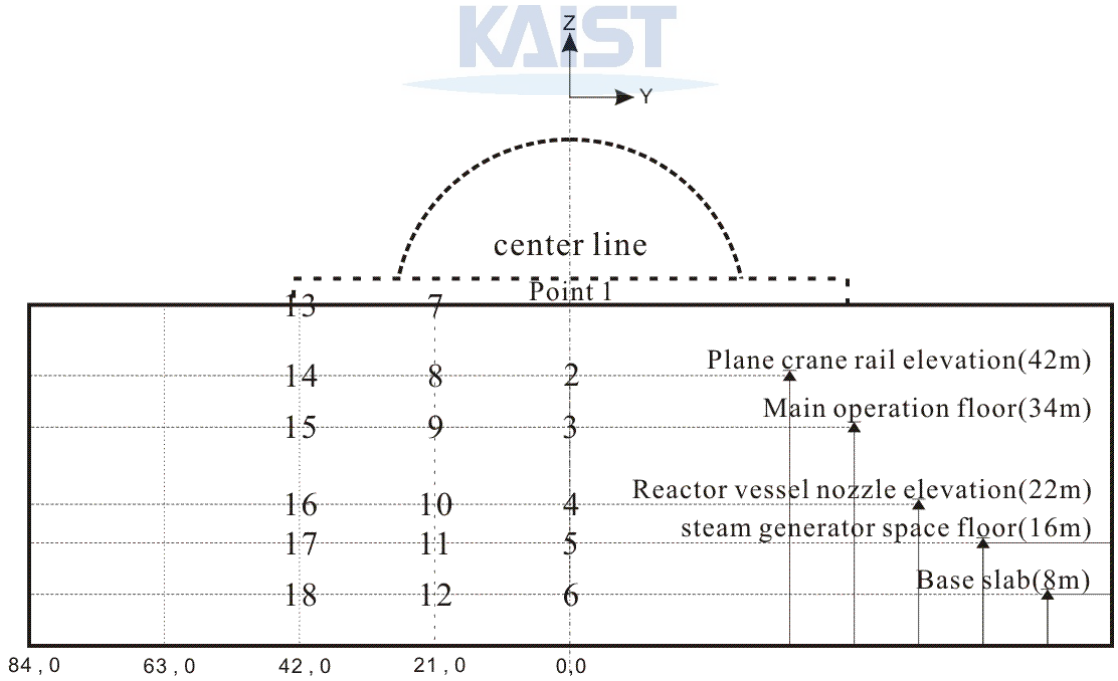

Fig. 22. Important station to obtain acceleration response

Usually the base isolation systems are applied to the NPP to increase safety of NPP during earthquake. There are two main purpose of base isolation system. The main idea of base isolation system is that to decrease the fundamental frequency of structure is

made lower than the predominant frequency of ground motion. The other purpose of base isolation system is to give energy dissipation by certain device or using natural phenomenon, reducing the transmitted acceleration into the superstructure. In case of GBS, the bottom is fixed to the seabed by using skirt to prevent sliding motion against wave loading or ocean current. However, the skirt is designed to yield under the severe earthquake due to prevent collapse of anchorage. Hence, after yielding of skirt, GBS is sliding with friction condition and decoupled from the seabed, which state is similar like friction base isolation system and in this study we will call such friction condition is pure-friction sliding condition. The pure-friction system is governed by frictional force between GBS bottom and seabed and friction force is function of coefficient of friction and total weight of superstructure. Therefore, by using characteristic of GBS ballasting system, which control the total weight of GBS, analysis of dynamic acceleration response according to change of GBS total weight have been conducted in present study. Addition to the change of GBS total weight, changing the coefficient of friction has been also used as variable to analyze the acceleration response of GBS. In the following chapter, the acceleration response is described with time and frequency domain.

5.2.1 Change of total weight of GBS for numerical experimental analysis

To study dynamic acceleration responses of GBS according to change of GBS, reinforced concrete unit density, dimension of GBS type ONPP and total SMART plant facilities weight information study have to be preceded. From the suggested concept design of GBS type ONPP, we can approximately calculate total weight of GBS type ONPP. The detail weight and dimension information of GBS type ONPP is described in Table 10 and 11.

Table. 10. Weight information of SMART`s main facilities and total weight

SMART 1 unit weight information	unit : ton
Reactor building	60,000
Auxiliary building	110,000
Compound building	75,000
Turbine & generator building	140,000
Inner facilities	12,000
Basemat / containment external	12,000

Other facilities	40,000
Total weight of single unit SMART	449,000

Table. 11. Total weight and Equivalent unit weight of GBS type ONPP & buoyancy

Total weight of GBS type ONPP (Total SMART weight + Total GBS weight + Ballasting)	1,101,450 ton
Applied buoyancy to the GBS	8,300,000 kN
Equivalent unit weight of GBS type ONPP	0.812 ton/m^3

The calculated total weight of GBS type ONPP is 1,101,450 ton. Based on this total weight information we can obtain the equivalent unit weight of GBS, which value is calculated by divide total weight by total volume of GBS. The calculated equivalent unit weight of GBS type ONPP is 0.8118 ton / m^3. In this study, we will use this equivalent unit weight as a default value for numerical experimental analysis. Addition to 812 kg/m^3, four unit weights are selected, which are 912,712,612 and 580 kg / m^3. The reason of using 580 kg/m^3 instead of 512 kg/m^3 is that buoyancy is bigger than the total weight of GBS type ONPP, if we use the 512 kg/m^3 as an equivalent unit weight. In real, buoyancy is applied to the GBS and lifting-up force is acting on the GBS. In this study, to reflect the buoyancy effects which acting on the GBS, artificial lifting-up force is imposed at the bottom of GBS in GBS-seawater-soil FE model. Submerged area of GBS is $168\text{m (W)} \times 168\text{m(L)} \times 30\text{m(H)}$ and obtained buoyancy is approximately 8,300,000 kN(= 294,000 Pa) when using 1000 kg/m^3 and 9.8 m/sec^2 as a unit weight of seawater and acceleration due to gravity, respectively. In other word, to maintain bottoming state of GBS, the limit equivalent unit weight of GBS type ONPP is 566 kg/m^3.

Using these five equivalent unit weight (912, 812, 712, 612 and 580 kg/m3) as analysis variables dynamic analysis has been conducted under the selected four ground motion (harmonic, Kobe, Elcentro and Tabas earthquake) by ADINA.

5.2.2 Change of coefficient of friction for numerical experimental analysis

Addition to the change of total weight of GBS type ONPP, coefficient of friction between GBS bottom and seabed has an effect on the dynamic behavior of GBS type

ONPP. GBS is commonly constructed by reinforce concrete and seabed condition is assumed in chapter 3.1.1. Also, ideal Coulomb fiction is used for the interface between GBS bottom and seabed. Usually, coefficient of friction is used 0.5 for the concrete and rough soil. However, in this study, we assumed that soil condition is fully saturated and water interface exists between GBS bottom and seabed, the default coefficient of friction is selected as 0.4. To verify effects of change of friction coefficient, addition to the 0.4, three more values (0.3, 0.2 and 0.1) are selected for the numerical experimental analysis. In this study, we regarded that coefficient of static friction and coefficient of kinetic friction is same.

Using selected coefficient of friction (0.4, 0.3, 0.2, and 0.1) as an analysis variable for dynamic analysis has been implemented under the selected four ground motion (harmonic, Kobe, Elcentro and Tabas earthquake) by ADINA. Also, to show the base isolation effects of pure-friction against bottom fixed condition, the acceleration response results from pure-friction and fixed condition are compared in the following chapter.

Chapter 6. Results and discussion

6.1 Acceleration response analysis according to unit weight change

Before analyzing acceleration response under the real earthquake; Kobe, El-centro, and Tabas, preliminary the acceleration response during harmonic ground motion need to be discussed to clearly verify the effect of acceleration response according to change of total weight of GBS using ADINA. Under the harmonic ground motion, the numerically computed horizontal acceleration at the selected important stations; point 1, point3 and point5 are as shown in Figure 23. In the Figure 23, acceleration results of unit weight density 912, 712 and 580 kg/m^3 are plotted with the purpose of preventing complexity of view and GBS bottom and seabed contact condition is friction using 0.4 as a Coefficient of friction.

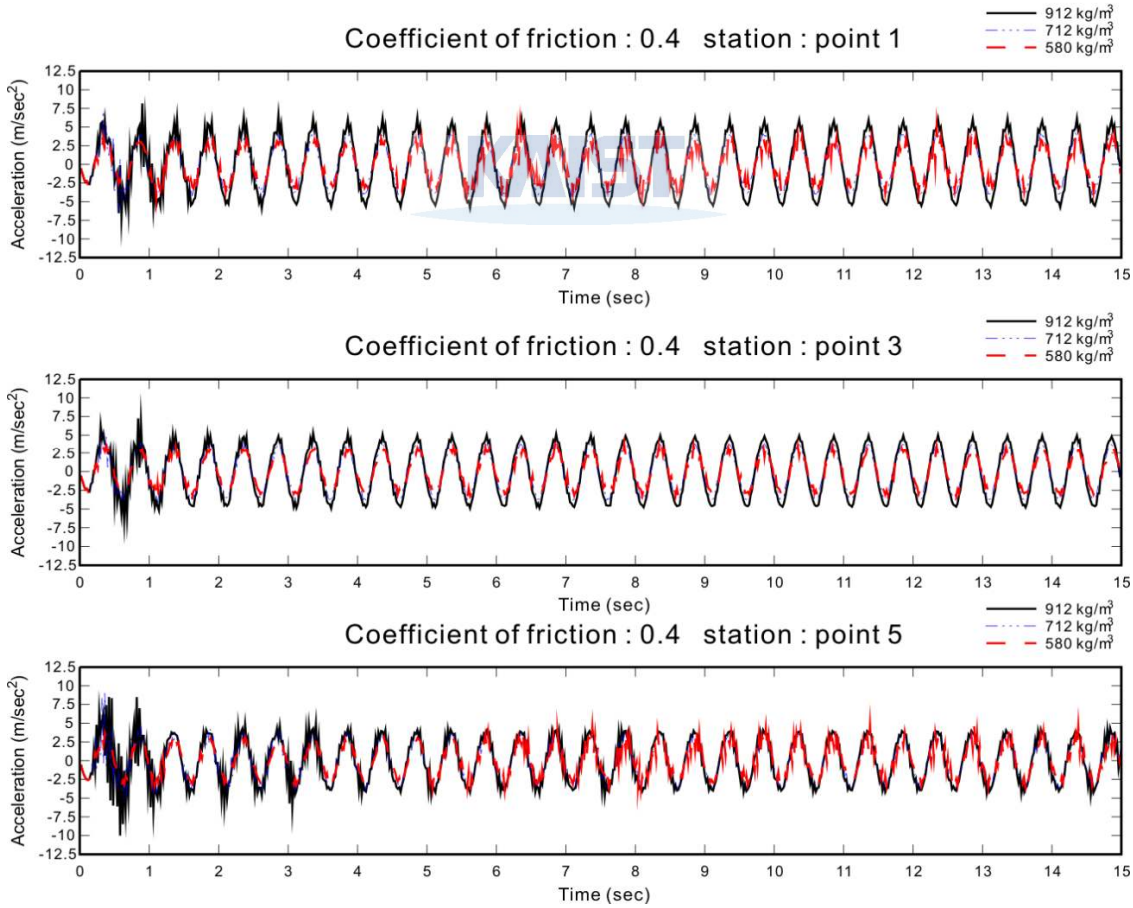

Fig. 23. Horizontal acceleration response in time domain during harmonic ground motion according to change of unit weight: point 1, 3 and 5, coefficient of friction: 0.4

It is evident that the acceleration response is reduced by decreasing unit weight of GBS during harmonic ground motion and the acceleration response also has tendency of harmonic. Physically, when superstructure`s weight is decreasing, the lateral sliding motion is easily occurred and transferred earthquake acceleration is reduced due to reduction of structure inertia. In other word, the GBS bottom is easily decoupled from the seabed, the transferred earthquake acceleration is decreased.

The absolute maximum horizontal acceleration comparing results according to change of unit weight of GBS type ONPP is shown as Table 12 and Figure 24 during harmonic ground motion. When we compare the absolute maximum acceleration response, at the point 5, 912 kg/m^3 case absolute maximum acceleration is 10.0 m/sec^2 and 580 kg/m^3 case is 4.76 m/sec^2, that is almost 52% decreased. The peak acceleration response is occurred within 1 second of time domain because the sliding motion of GBS is occurred right after when the generated frictional force by earthquake is bigger than the normal force by total weight of GBS type ONPP. Especially, the result from point 5 shows that right after significant acceleration response occur within one second, the acceleration response is much smaller and maintain certain acceleration. After beginning of sliding motion of GBS, acceleration responses are similar in the range of entire time domain, but we can observe the acceleration reducing effects according to change of unit weight of GBS type ONPP under the harmonic ground motion.

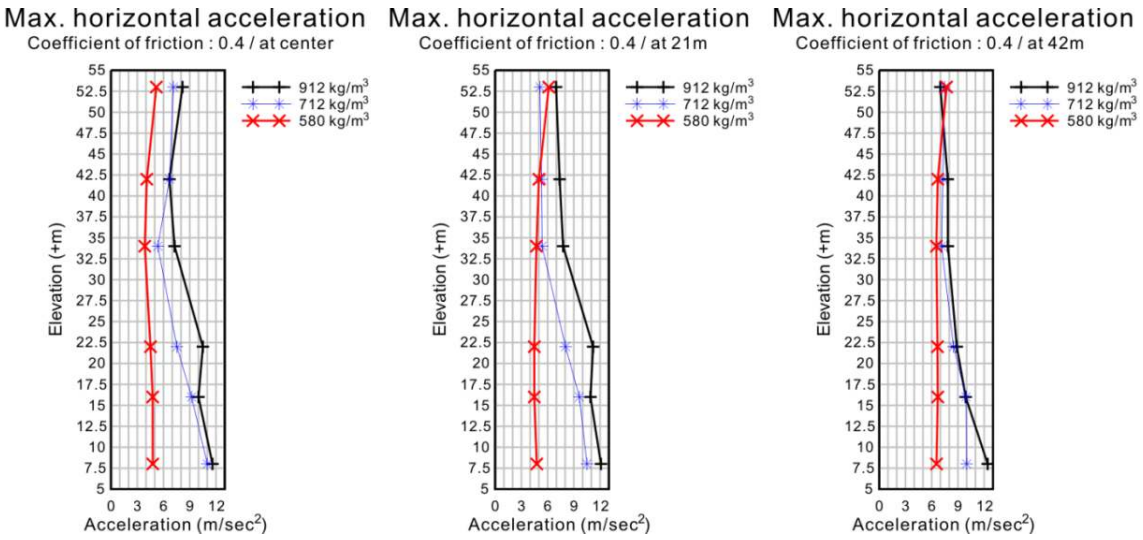

Fig. 24. Comparing absolute maximum horizontal acceleration during harmonic ground motion according to change of unit weight

Table. 12. Absolute maximum horizontal acceleration according to change of unit weight at selected eighteen stations during harmonic ground motion

Coefficient of friction : 0.4						acceleration unit : m/ sec^2
Unit weight : 912 kg/m^3						
Position	53m	42m	34m	22m	16m	8m
0 m	8.17	6.68	7.26	10.5	10	11.6
21 m	6.97	7.38	7.77	11.2	10.9	12.1
42 m	6.98	7.84	7.85	8.87	9.88	12.4
Unit weight : 712 kg/m^3						
0 m	7.14	6.69	5.36	7.53	9.22	11
21 m	5.12	5.3	5.37	8.05	9.63	10.5
42 m	7.49	7.26	7.13	8.5	9.92	10
Unit weight : 580 kg/m^3						
0 m	5.18	4.09	3.86	4.51	4.76	4.77
21 m	6.13	5.01	4.72	4.48	4.48	4.76
42 m	7.7	6.69	6.53	6.66	6.69	6.55

In this study, addition to the analysis of acceleration response in time domain and the absolute maximum acceleration, floor response spectra approach has also conducted to evaluate dynamic response of GBS type ONPP at the important elevation. The computed results of FRS under the harmonic ground motion are shown as Figure 25. FRS approach has been also implemented according to change of unit weight of GBS. The examination of response spectra indicates that there is progressive increase in response going from the point 5 to point 1. Addition to the progressive increase of floor acceleration, the effects of change of unit weight of GBS is clearly observed in the FRS as show in Figure 25. By decreasing of unit weight, the peak response amplification of FRS is also reduced near the 2 Hz region. The dominant frequency of harmonic ground motion is 2Hz. Especially, at the top of GBS, which location is point 1 in FE model, reducing of the peak response amplification is more clearly observed.

Through numerically computed horizontal acceleration response in time domain during harmonic ground motion, we can verify the acceleration reducing effects according to change of unit weight of GBS, so far. Addition to the harmonic ground motion, dynamic response analysis has been conducted also during selected real-earthquake; Kobe, El-centro and Tabas.

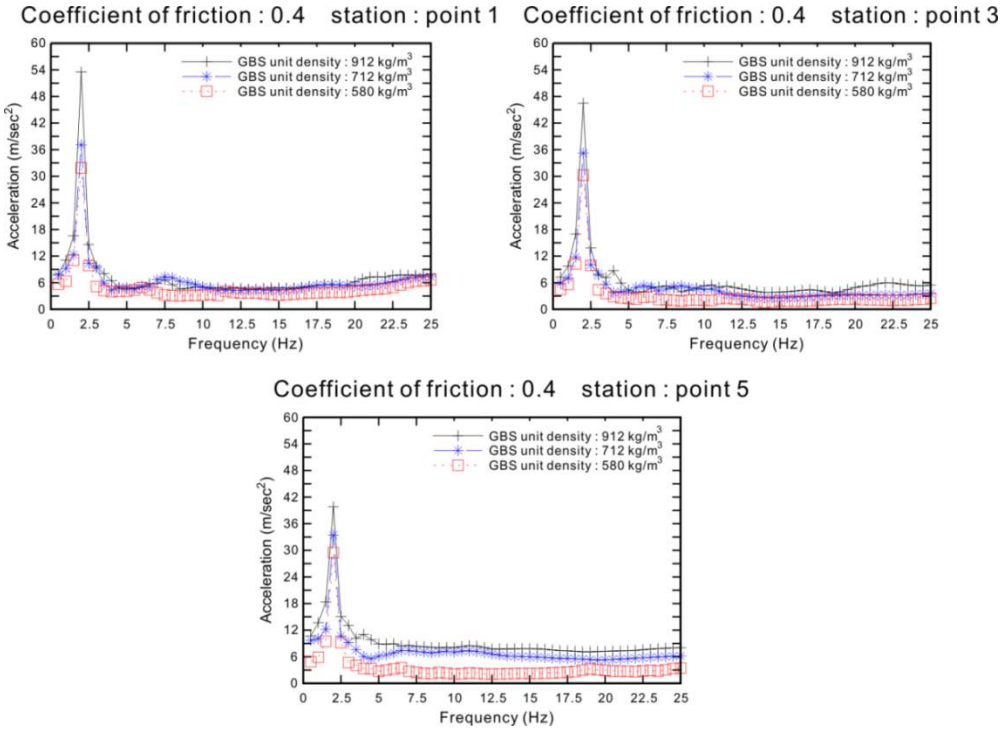

Fig. 25. Floor response spectra of point 1, 3 and during harmonic ground motion according to change of unit weight

The horizontal acceleration responses in time domain during Kobe earthquake are depicted in Figure 26. In contradiction to the harmonic ground motion, the acceleration response according to change of unit weight of GBS is not significantly observed. Also, at the point 1, the absolute maximum horizontal acceleration case of 580 kg/m^3 is bigger than 912 kg/m^3 case as described in Table 13. Such phenomenon is also observed in the Tabas results in Table 12. By reducing unit weight of GBS, the inertia of structure is reduced. As a result, GBS is easily decoupled and sliding from and above seabed. However, according to decrease of superstructure`s inertia, the relative motion of structure can be increased at the top or end of the structure. When we consider the very huge structure model, the acceleration response is not same entire region of structure. Relatively, the end side or tip part of structure`s acceleration is bigger than center of structure, if the structure is not rigid. In this study, the used GBS FE model is not rigid and instead of lumped model, we used full mass matrix for the structure FE model and seabed is modeled by Mohr-Coulomb plastic model. Also, Kobe and Tabas is relatively severe earthquake than El-centro and harmonic ground motion and irregular wave besides frictional contact condition is also considered. It is hard to explain such specific

phenomenon under complex, irregular and non-linear condition. Hence, instead of focusing on the results of certain point, the entire acceleration responses reduction effects in time domain regard as the main purpose of this study. In this sense, at the point 3 and 5, the reduction of absolute maximum horizontal acceleration is observed during Kobe and Tabas earthquake as shown in Table 13 and 15. Also, reduction of horizontal acceleration response in time is observed during Kobe, El-centro and Tabas as depicted in Figure 26, 29 and 32. Also, FRS shows that the reduction of peak response amplification is observed in Figure 28, 31 and 34.

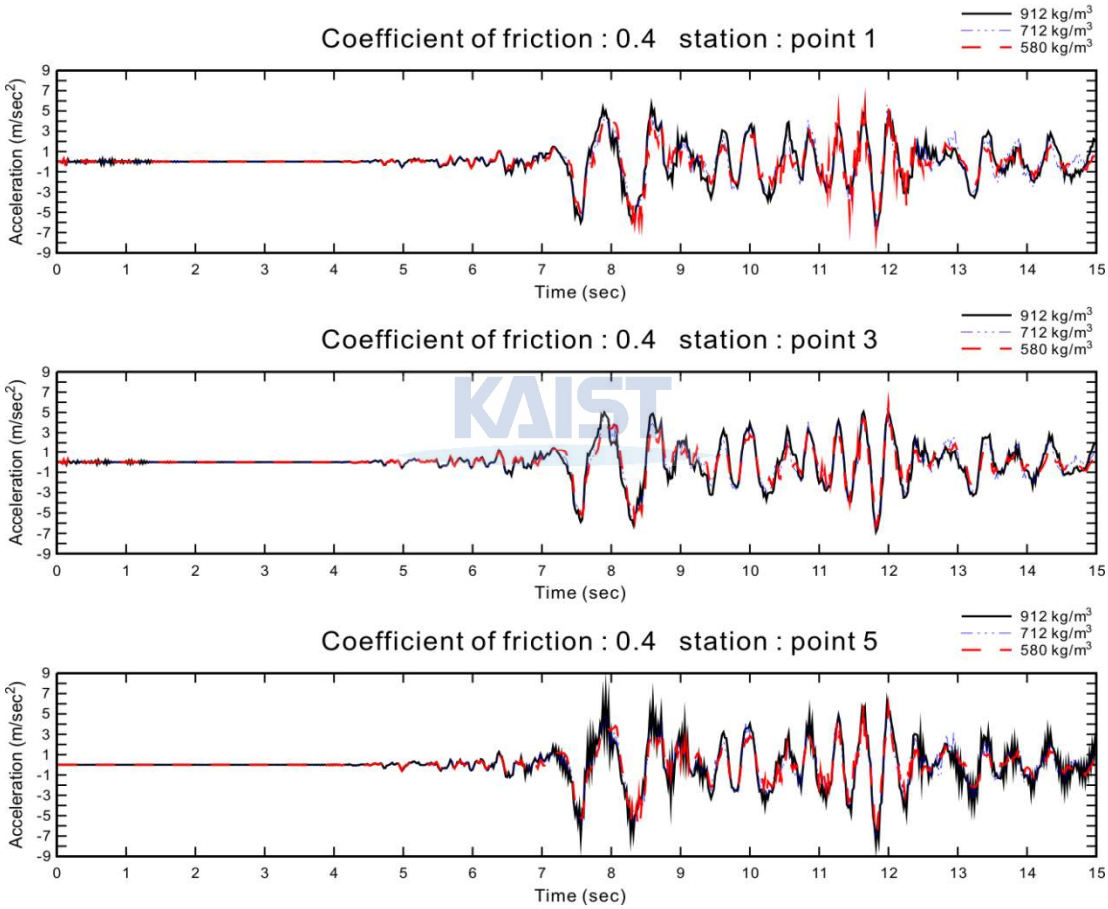

Fig. 26. Horizontal acceleration response in time domain during Kobe earthquake according to change of unit weight: point 1, 3 and 5, coefficient of friction: 0.4

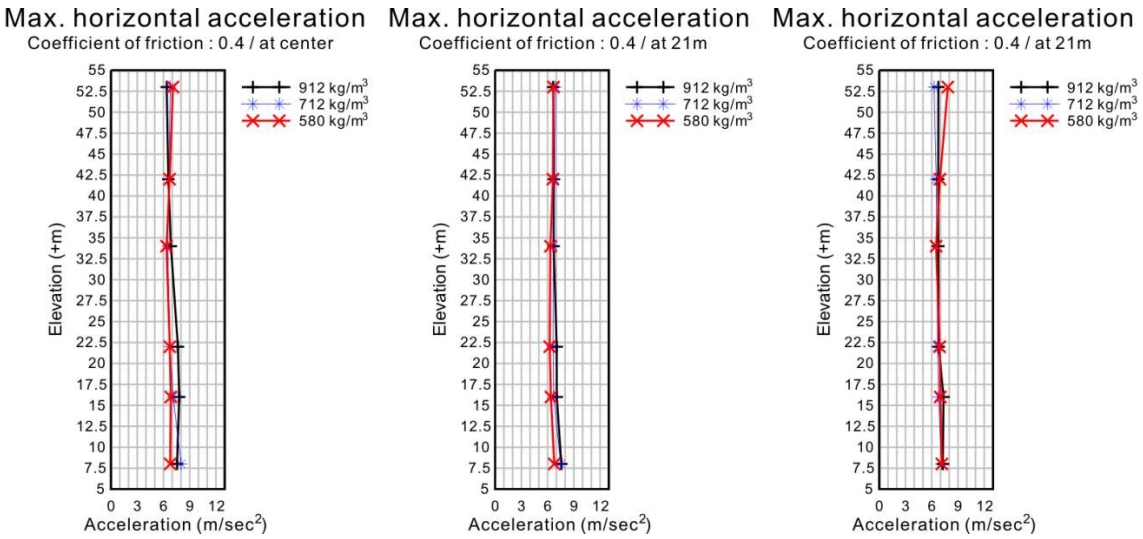

Fig. 27. Comparing absolute maximum horizontal acceleration during Kobe earthquake according to change of unit weight

Table. 13. Absolute maximum horizontal acceleration according to change of unit weight at selected eighteen stations during Kobe earthquake

Coefficient of friction : 0.4					acceleration unit : m/ sec^2	
Unit weight : 912 kg/m^3						
Position	53m	42m	34m	22m	16m	8m
0 m	6.37	6.56	6.85	7.65	7.8	7.55
21 m	6.64	6.7	6.69	7.04	7.05	7.57
42 m	6.76	6.74	6.75	6.8	7.34	7.27
Unit weight : 712 kg/m^3						
0 m	6.78	6.63	6.49	6.74	7.1	8.01
21 m	6.9	6.78	6.64	6.64	6.7	7.48
42 m	6.27	6.51	6.58	6.67	6.79	7.1
Unit weight : 580 kg/m^3						
0 m	7.08	6.7	6.35	6.72	6.84	6.77
21 m	6.67	6.6	6.32	6.24	6.38	6.67
42 m	7.84	6.94	6.5	6.91	6.99	7.16

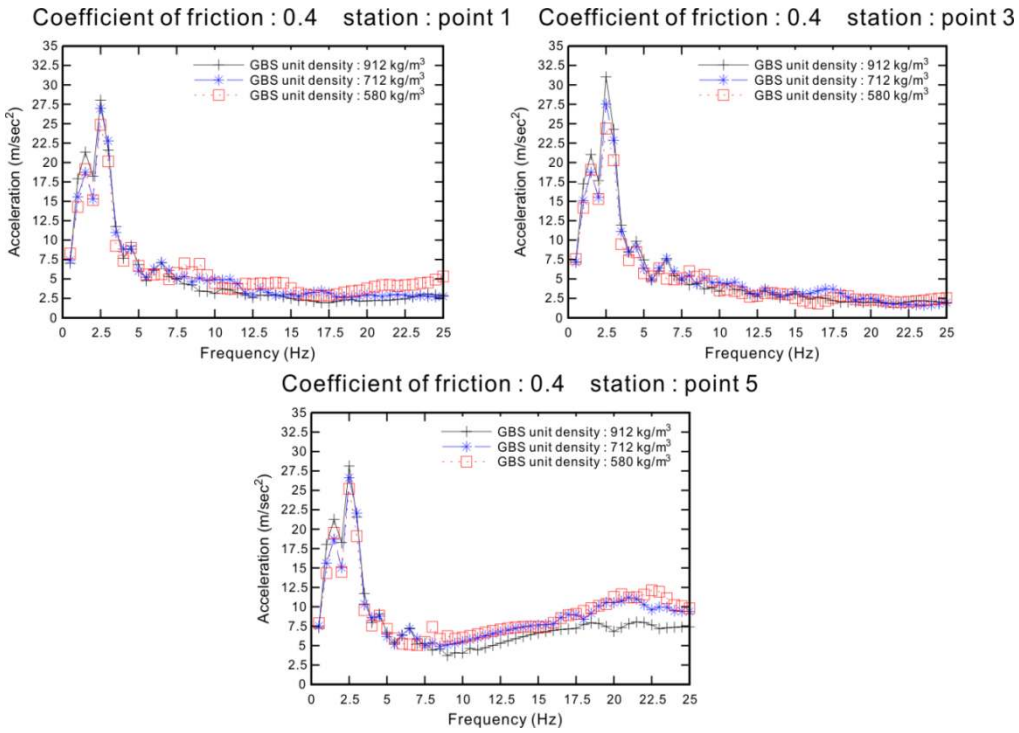

Fig. 28. Floor response spectra of point 1, 3 and 5 during Kobe earthquake according to change of unit weight

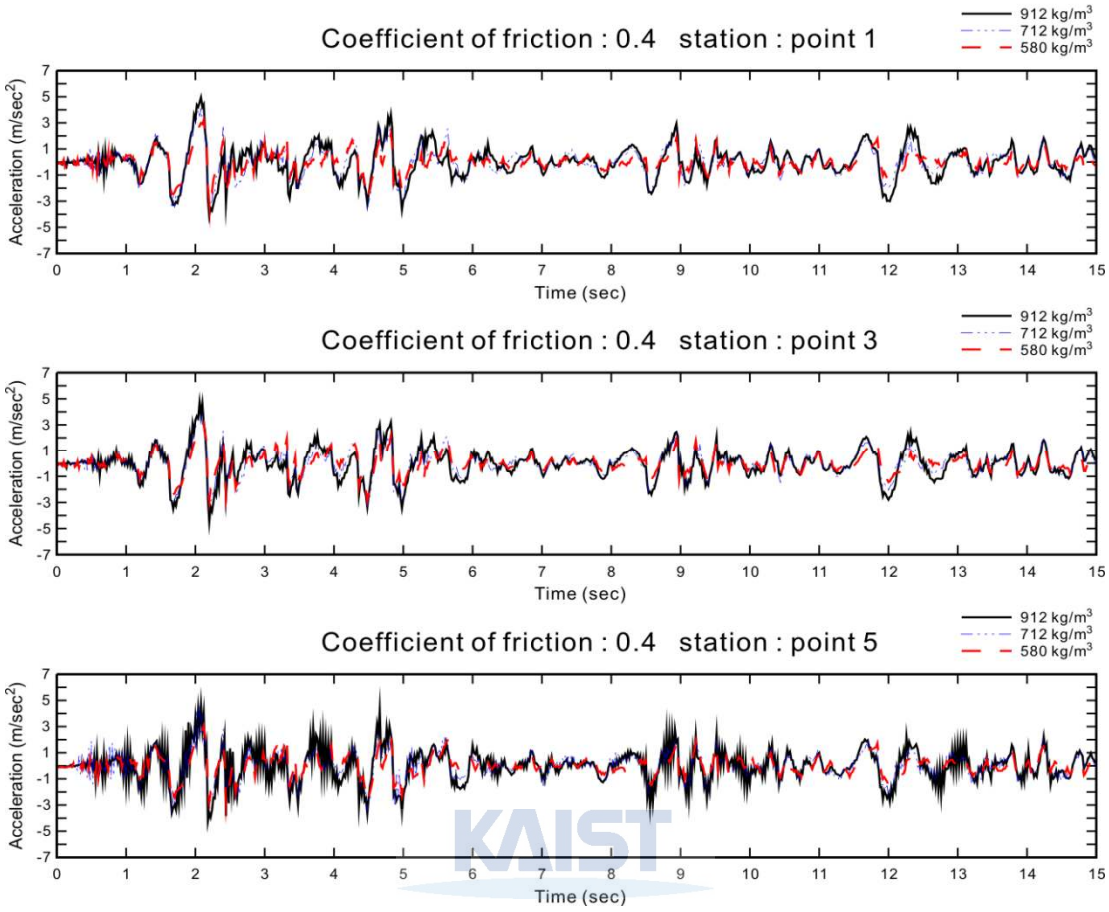

Fig. 29. Horizontal acceleration response in time domain during El-centro earthquake according to change of unit weight: point 1, 3 and 5, coefficient of friction: 0.4

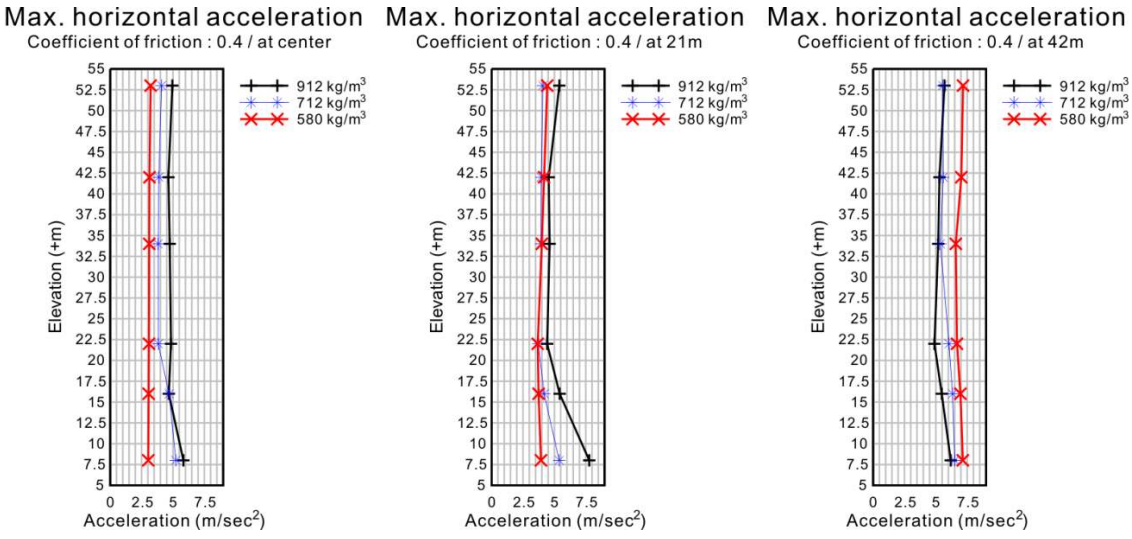

Fig. 30. Comparing absolute maximum horizontal acceleration during El-centro earthquake according to change of unit weight

Table. 14. Absolute maximum horizontal acceleration according to change of unit weight at selected eighteen stations during El-centro earthquake

Coefficient of friction : 0.4						acceleration unit : m/ sec^2
Unit weight : 912 kg/m^3						
Position	53m	42m	34m	22m	16m	8m
0 m	4.95	4.64	4.74	4.84	4.67	5.83
21 m	5.39	4.55	4.62	4.42	5.42	7.78
42 m	5.69	5.29	5.19	4.89	5.47	6.19
Unit weight : 712 kg/m^3						
0 m	4.09	3.87	3.82	3.83	4.69	5.23
21 m	4.08	3.95	3.93	3.72	4.18	5.38
42 m	7.13	6.67	6.69	6.88	6.86	7.61
Unit weight : 580 kg/m^3						
0 m	3.22	3.13	3.09	3.09	3.06	3.03
21 m	4.43	4.18	4	3.67	3.74	3.93
42 m	7.17	7.03	6.59	6.69	6.96	7.15

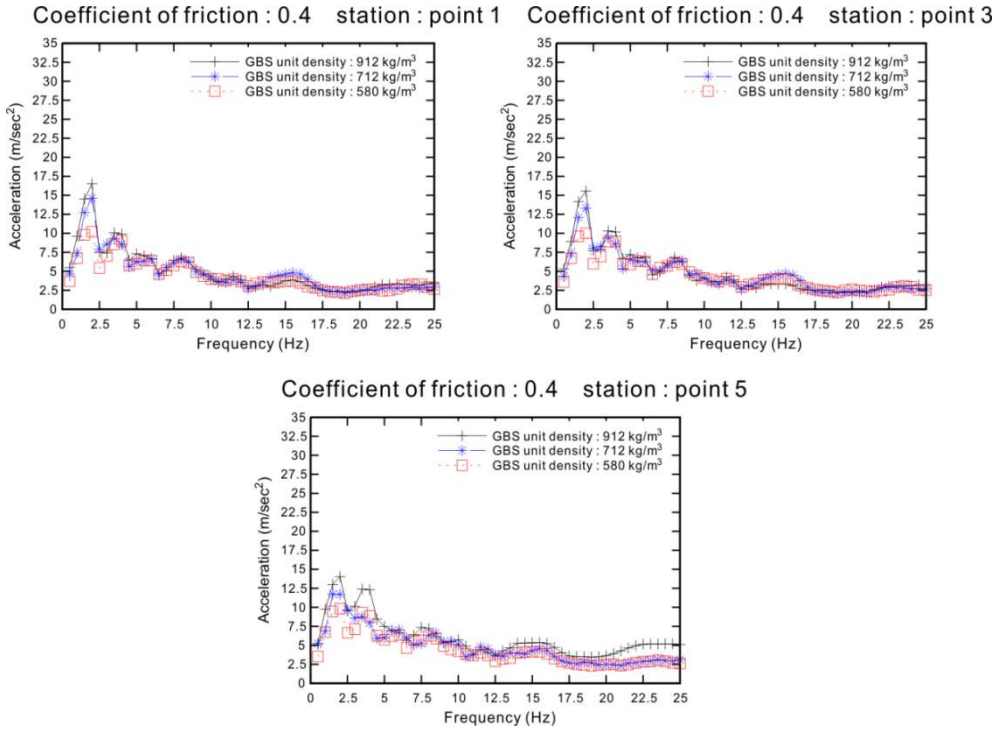

Fig. 31. Floor response spectra of point 1, 3 and 5 during El-centro earthquake according to unit

weight change

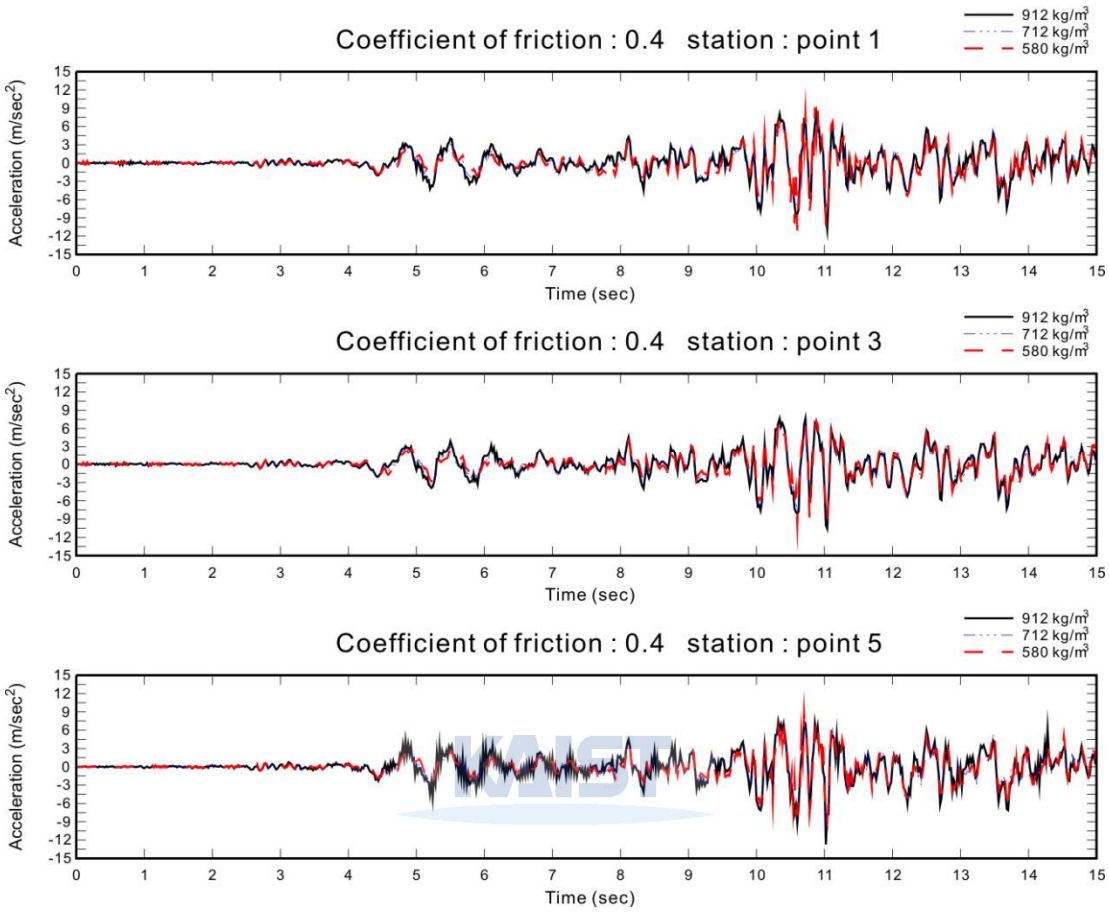

Fig. 32. Horizontal acceleration response in time domain during Tabas earthquake according to unit weight change: point 1, 3 and 5, coefficient of friction: 0.4

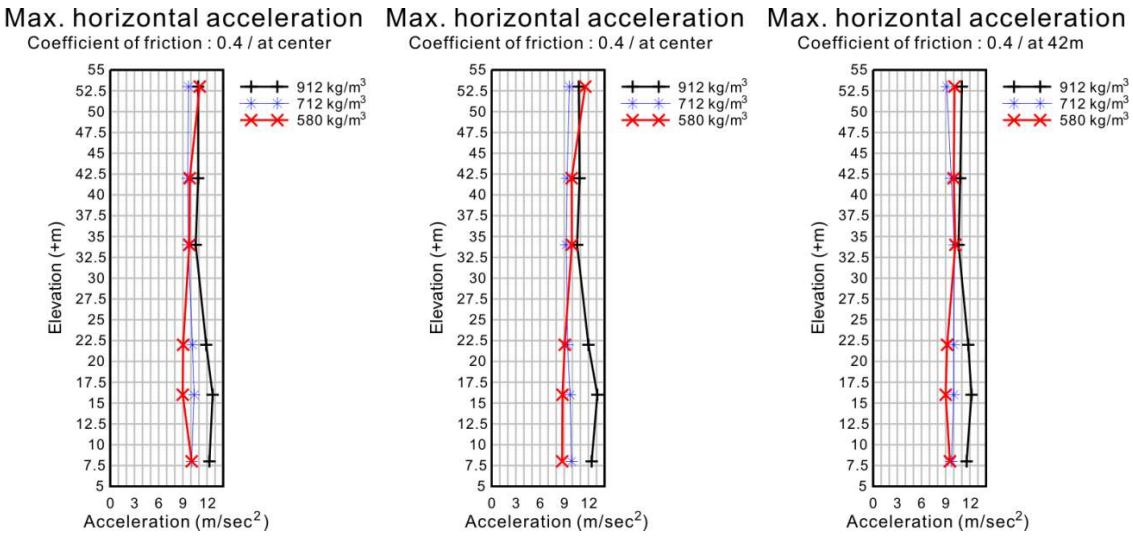

Fig. 33. Comparing absolute maximum horizontal acceleration during Tabas earthquake

according to unit weight change

Table. 15. Absolute maximum horizontal acceleration according to change of unit weight at selected eighteen stations during Tabas earthquake

Coefficient of friction : 0.4						acceleration unit : m/ sec^2
Unit weight : 912 kg/m^3						
Position	53m	42m	34m	22m	16m	8m
0 m	10.9	10.9	10.6	11.9	12.7	12.3
21 m	10.8	10.9	10.6	12	13.1	12.4
42 m	11	10.8	10.6	11.8	12.2	11.6
Unit weight : 712 kg/m^3						
0 m	9.71	9.61	9.67	10.2	10.4	10.1
21 m	9.64	9.35	9.24	9.42	9.72	9.89
42 m	9.13	9.69	10.1	10	10	9.72
Unit weight : 580 kg/m^3						
0 m	11.1	9.86	9.8	9.04	8.99	10.1
21 m	11.6	9.92	9.94	9.06	8.78	8.74
42 m	10.1	10	10.2	9.18	9	9.52

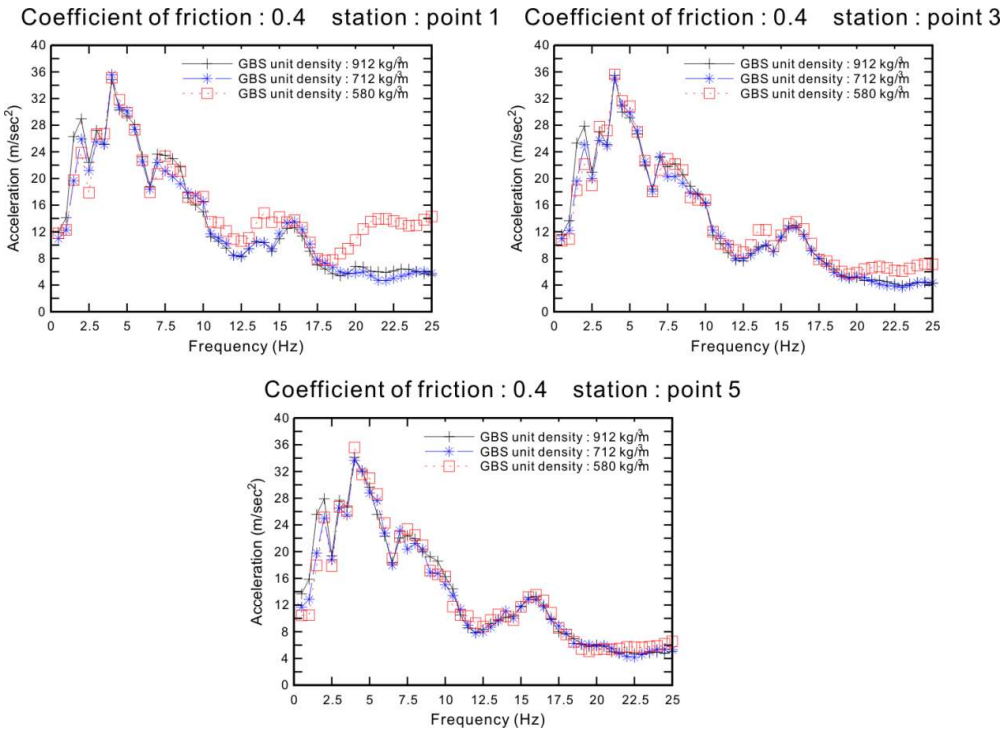

Fig. 34. Floor response spectra of point 1, 3 and 5 during Tabas earthquake according to unit weight change

When we study acceleration responses during Tabas, it is hard to see significant acceleration reduction according to change of unit weight of GBS. The horizontal peak ground acceleration (PGA) of Tabas earthquake is 0.852g as described in Table 8. Tabas earthquake is almost three times bigger than harmonic and El-centro earthquake. Under the extreme earthquake like Tabas, the acceleration reduction effects according to change of unit weight is insignificant. This phenomenon is also observed in the FRS results as shown in Figure 34. The peak amplitude case of 912, 712, 580kg/m3 is almost same in frequency range of 3.5~4.5 Hz.

6.2 Acceleration response analysis according to Coefficient of friction change

As mentioned before, the total weight of GBS is changeable with ballasting system. In chapter 6.1, the acceleration reduction effects of GBS type ONPP according to unit weigh change of superstructure is discussed. In this chapter, addition to the unit weight change, by using change of coefficient of friction between GBS bottom and seabed, acceleration response reduction effects is demonstrated. For the analysis, 0.4, 0.3, 0.2 and 0.1 values are selected as analysis variable of coefficient of friction.

By following analysis procedure of unit weight change, firstly, dynamic response analysis has been conducted under harmonic ground motion. The horizontal acceleration responses and reduction effects according to friction coefficient change are shown in Figure 35. As a default unit weight, the 912 kg/m^3 is used for analysis. According to decreasing of coefficient of friction, horizontal acceleration responses are reduced in time history. The reason is that delivered earthquake load is reduced due to superstructure easily decoupled and sliding from and above the seabed by using small coefficient of friction. As described in Table 16, the peak acceleration of 0.4 and 0.1 cases at point 5 and point 1, almost 50% reduction is observed during harmonic ground motion. The maximum horizontal acceleration responses results of friction coefficient change are plotted in Figure 36.

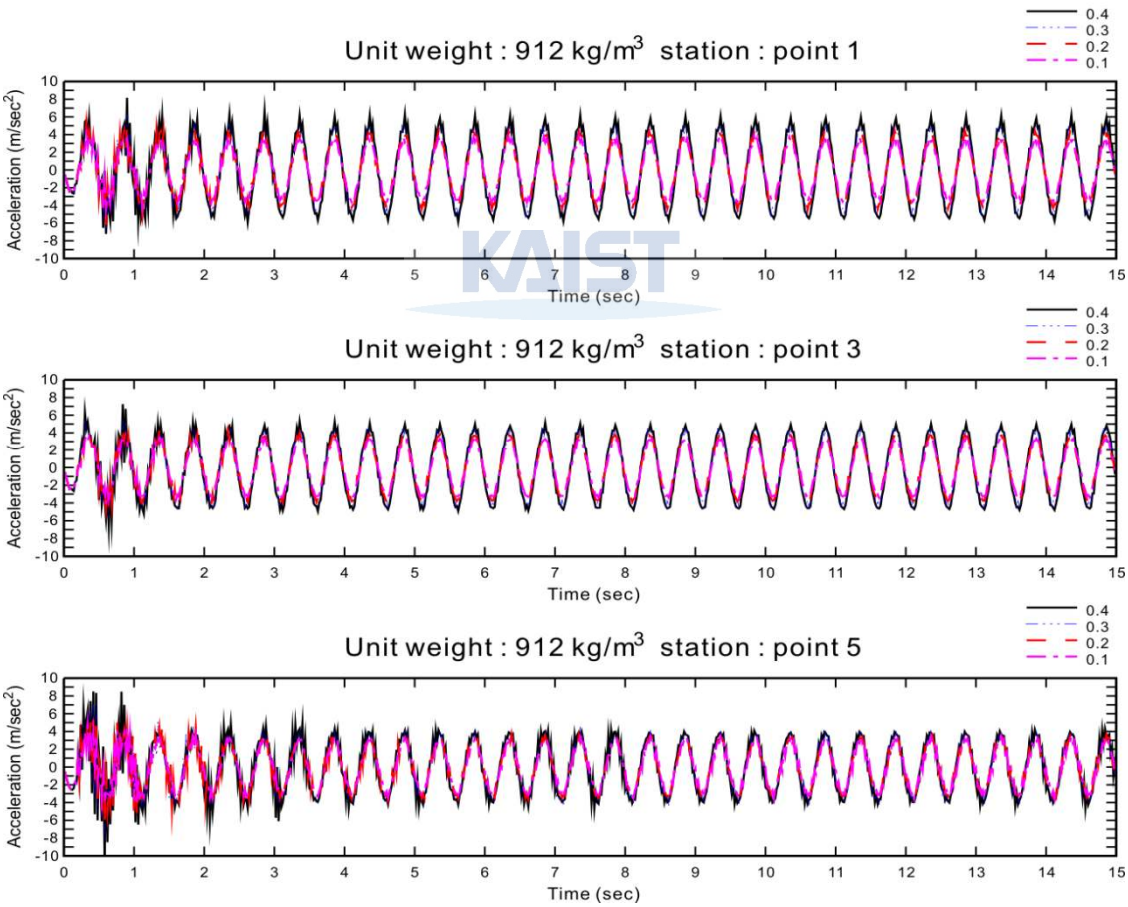

Fig. 35. Horizontal acceleration response in time domain during harmonic ground motion according to change of friction coefficient: point 1, 3 and 5, Unit weight: 912 kg/m^3

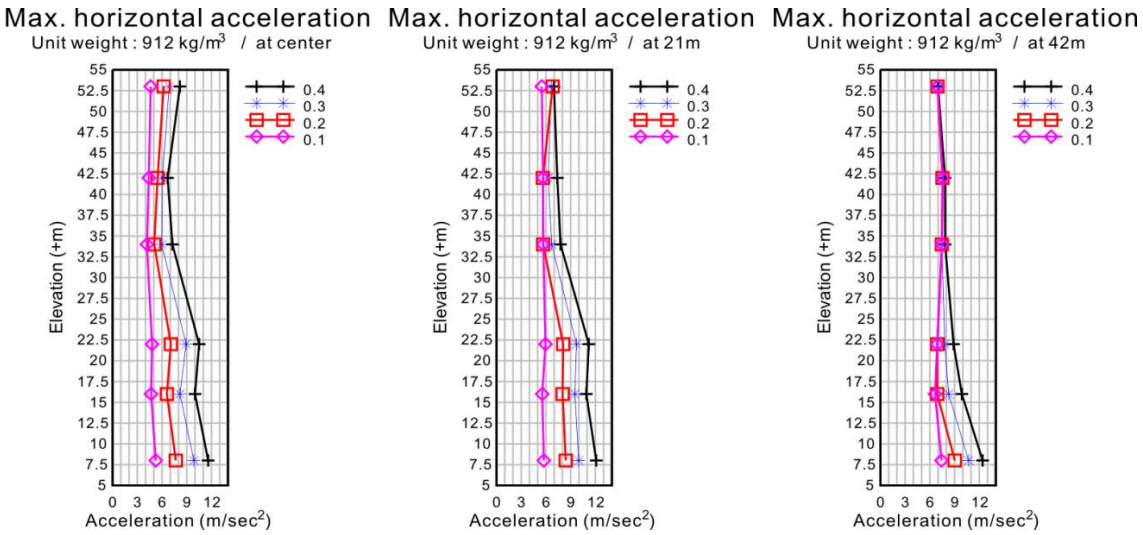

Fig. 36. Comparing absolute maximum horizontal acceleration during harmonic ground motion according to friction coefficient change

Table. 16. Absolute maximum horizontal acceleration according to change of friction coefficient at selected eighteen stations during harmonic ground motion

Unit weight of GBS type ONPP : 912kg/m^3				acceleration unit : m/ sec^2		
Coefficient of friction : 0.4						
Position	53m	42m	34m	22m	16m	8m
0 m	8.17	6.68	7.26	10.5	10	11.6
21 m	6.97	7.38	7.77	11.2	10.9	12.1
42 m	6.98	7.84	7.85	8.87	9.88	12.4
Coefficient of friction : 0.3						
0 m	6.87	6.04	5.96	8.92	8.18	9.86
21 m	6.66	6.26	6.7	9.7	9.51	9.97
42 m	6.91	7.53	7.45	7.81	8.28	10.7
Coefficient of friction : 0.2						
0 m	6.2	5.46	5.06	7.07	6.59	7.67
21 m	6.81	5.63	5.66	8.09	8.02	8.4
42 m	6.92	7.53	7.45	6.9	6.89	9.02
Coefficient of friction : 0.1						
0 m	4.62	4.4	4.17	4.79	4.67	5.24
21 m	5.49	5.64	5.67	5.94	5.55	5.74
42 m	6.93	7.54	7.46	6.89	6.63	7.41

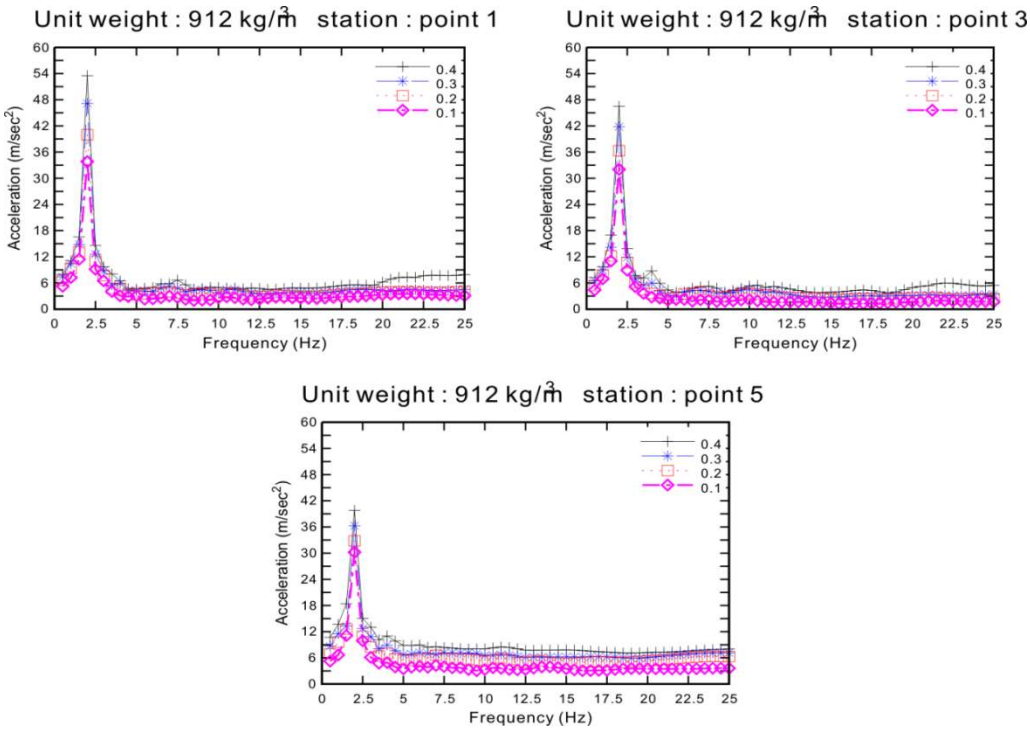

Fig. 37. Floor response spectra of point 1, 3 and 5 during harmonic ground motion according to friction coefficient change

As we expected, the horizontal acceleration reduction effects also are observed during Kobe, El-centro and Tabas earthquake according to change of friction coefficient and results in time domain are described in Figure 38, 41 and 44. When we compare the acceleration reduction effects between unit weight change and friction coefficient change by results of absolute maximum horizontal acceleration, the reduction effects are almost same during Kobe, El-centro and Tabas.

The results of FRS are shown in Figure 40, 43 and 46. Except Tabas case, the peak response amplification reduction effects are observed clearly. The peak responses amplification and dominant frequency region of unit weight change and friction coefficient change are almost same as shown in Table 20. It can be extracted from the results of all analysis cases that, the peak responses amplification is existed in near the 2.0 Hz exclude Tabas case. Through case of Tabas earthquake, one may realize the fact that, under the extreme earthquake, the acceleration reduction effects are insignificant according to change of friction coefficient and unit weight.

Based on these results, we can say that the acceleration reduction effects according to change of friction coefficient is as effective as unit weight change. However, in contradiction to unit weight change, absolute maximum acceleration reduction tendency is relatively regularity according to change of coefficient of friction and elevation of

GBS. These tendencies are also observed result of Kobe, El-centro and Tabas earthquake as shown in Figure 39, 42 and 45.

In this study, we used ideal Mohr-coulomb friction model to model interface between GBS bottom and seabed, which model is governed by coefficient friction and total weight of superstructure in ADINA. In case of friction coefficient, it has only an effect on the frictional force, but total weight of superstructure has effects on both frictional force and dynamic behavior of superstructure at the same time. When we compare the absolute maximum horizontal acceleration results of unit weight and friction coefficient change during El-centro earthquake at 42m location, there are no an unprecedented phenomenon in the results of friction coefficient change like unit weight change; 580 kg/m^3 maximum horizontal acceleration is bigger than 912 kg/m^3 because inertia effect due to change of unit weight is not reflected in the coefficient of friction change analysis. Hence, we could say that, control of coefficient of friction is more clear and easy to reduce the acceleration response from the perspective of academically approach.

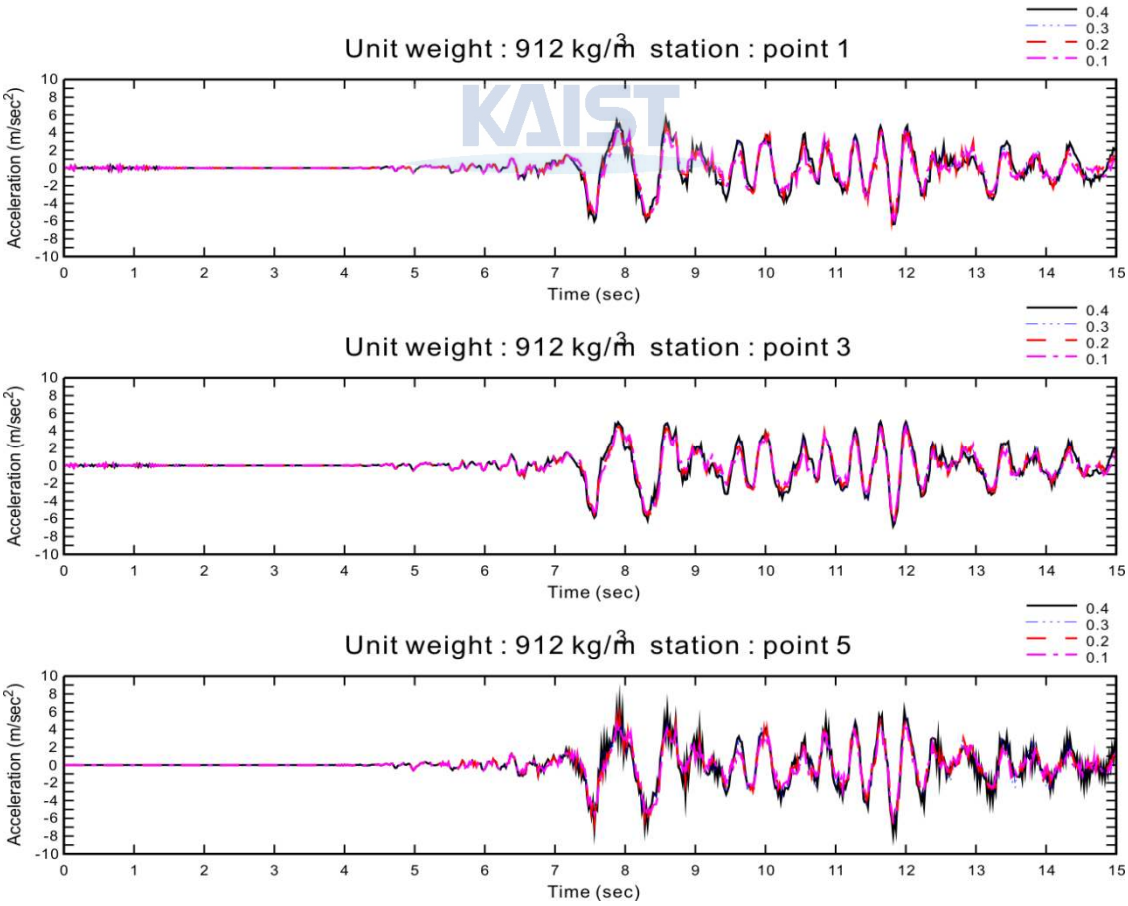

Fig. 38. Horizontal acceleration response in time domain during Kobe earthquake according to change of friction coefficient: point 1, 3 and 5, Unit weight: 912 kg/m3

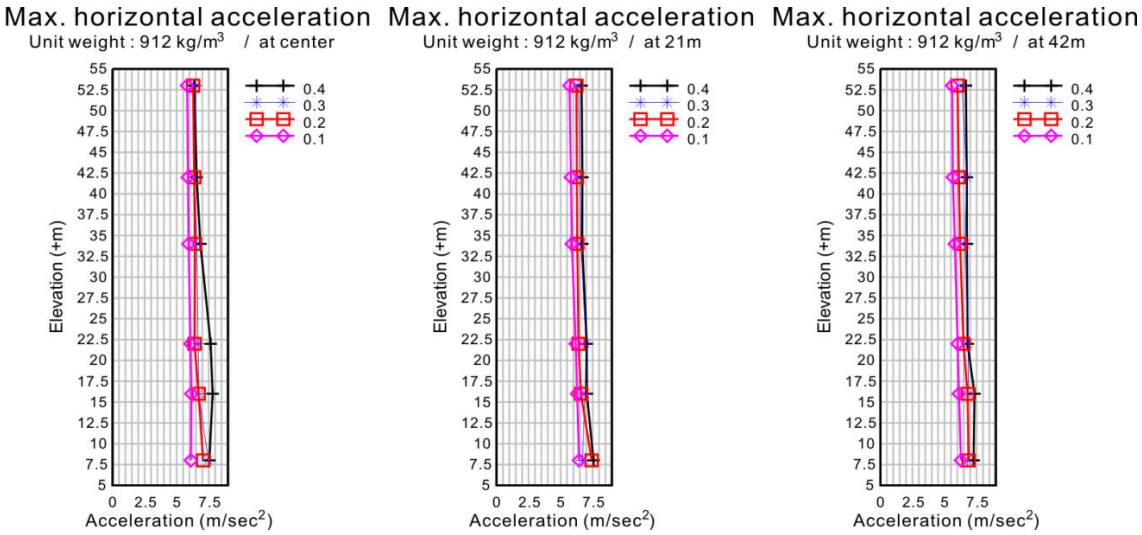

Fig. 39. Comparing absolute maximum horizontal acceleration during Kobe earthquake according to friction coefficient change

Table. 17. Absolute maximum horizontal acceleration according to change of friction coefficient at selected eighteen stations during Kobe earthquake

Unit weight of GBS type ONPP : 912kg/m^3				acceleration unit : m/ sec^2		
Coefficient of friction : 0.4						
Position	53m	42m	34m	22m	16m	8m
0 m	6.37	6.56	6.85	7.65	7.8	7.55
21 m	6.64	6.7	6.69	7.04	7.05	7.57
42 m	6.76	6.74	6.75	6.8	7.34	7.27
Coefficient of friction : 0.3						
0 m	6.47	6.38	6.58	6.67	6.73	7.47
21 m	6.38	6.53	6.58	6.98	6.91	6.71
42 m	6.38	6.72	6.59	6.84	6.86	6.81
Coefficient of friction : 0.2						
0 m	6.28	6.37	6.42	6.39	6.71	7.06
21 m	6.24	6.27	6.3	6.4	6.59	7.42
42 m	6.02	6.12	6.22	6.48	6.8	6.88
Coefficient of friction : 0.1						
0 m	5.82	5.88	5.93	6.08	6.15	6.11
21 m	5.7	5.81	5.88	6.18	6.29	6.45

42 m	5.6	5.65	5.81	6.03	6.12	6.29

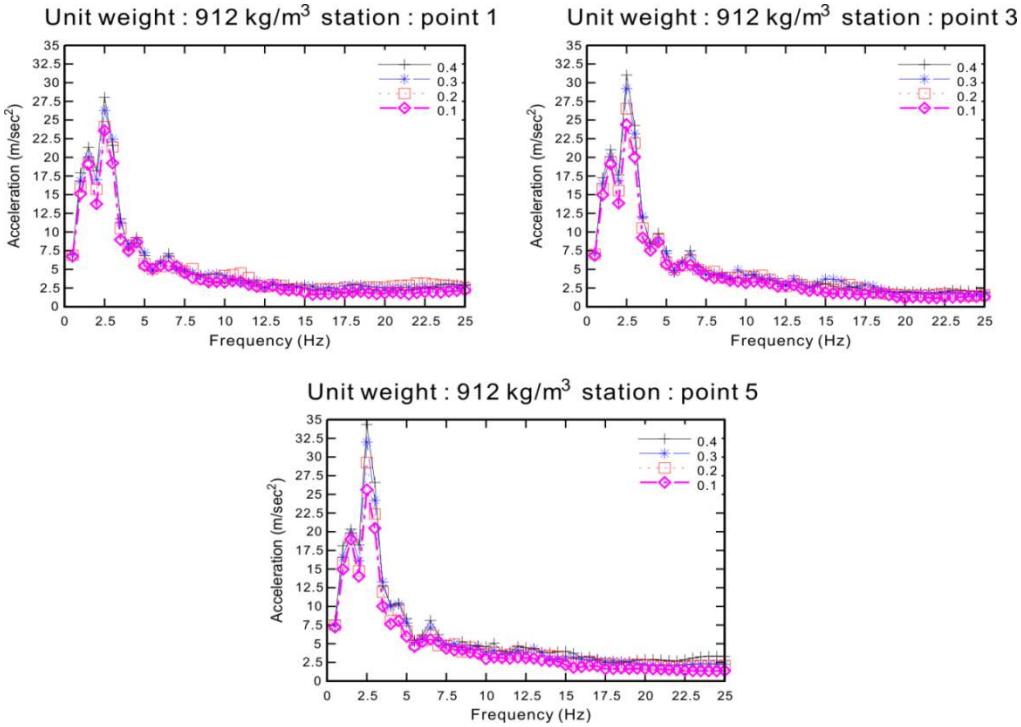

Fig. 40. Floor response spectra of point 1, 3 and 5 during Kobe earthquake according to friction coefficient change

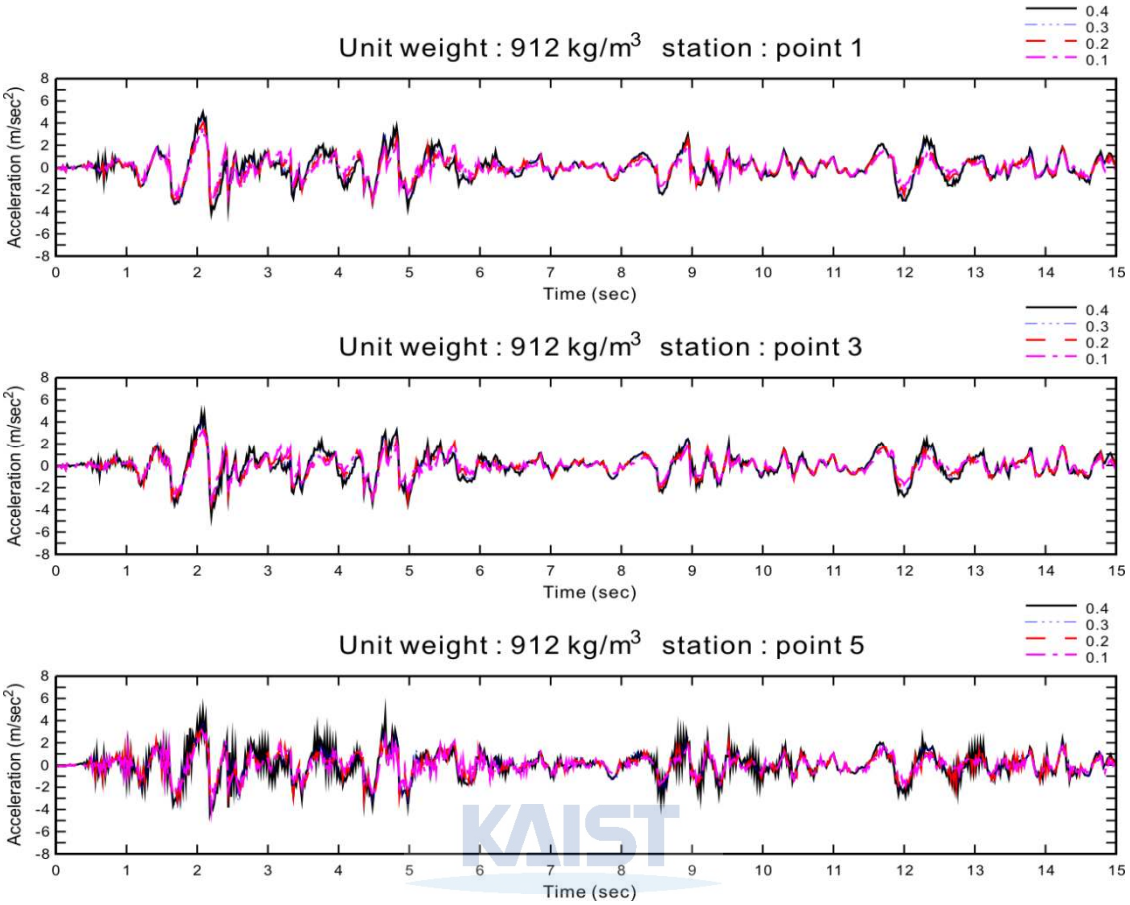

Fig. 41. Horizontal acceleration response in time domain during El-centro earthquake according to change of friction coefficient: point 1, 3 and 5, Unit weight: 912 kg/m3

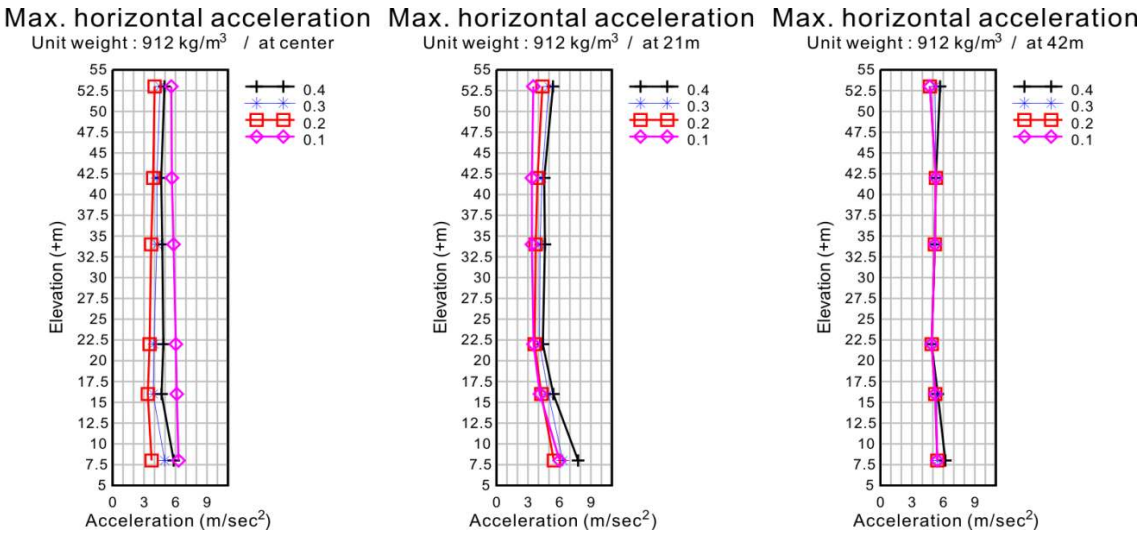

Fig. 42. Comparing absolute maximum horizontal acceleration during El-centro earthquake according to friction coefficient change

Table. 18. Absolute maximum horizontal acceleration according to change of friction coefficient at selected eighteen stations during El-centro earthquake

Unit weight of GBS type ONPP : 912kg/m^3					acceleration unit : m/ sec^2	
Coefficient of friction : 0.4						
Position	53m	42m	34m	22m	16m	8m
0 m	4.95	4.64	4.74	4.84	4.67	5.83
21 m	5.39	4.55	4.62	4.42	5.42	7.78
42 m	5.69	5.29	5.19	4.89	5.47	6.19
Coefficient of friction : 0.3						
0 m	4.53	4.22	4.23	3.94	3.87	4.97
21 m	4.99	4.34	4.15	4.11	4.95	6.32
42 m	5.2	5.29	5.19	4.89	5.39	5.43
Coefficient of friction : 0.2						
0 m	4.01	3.87	3.68	3.53	3.36	3.72
21 m	4.38	3.91	3.74	3.64	4.27	5.47
42 m	4.72	5.29	5.19	4.89	5.22	5.43
Coefficient of friction : 0.1						
0 m	3.58	3.4	3.22	3.57	3.72	3.52
21 m	3.51	3.38	3.38	3.53	4.14	6.02
42 m	4.72	5.29	5.19	4.89	5.22	5.43

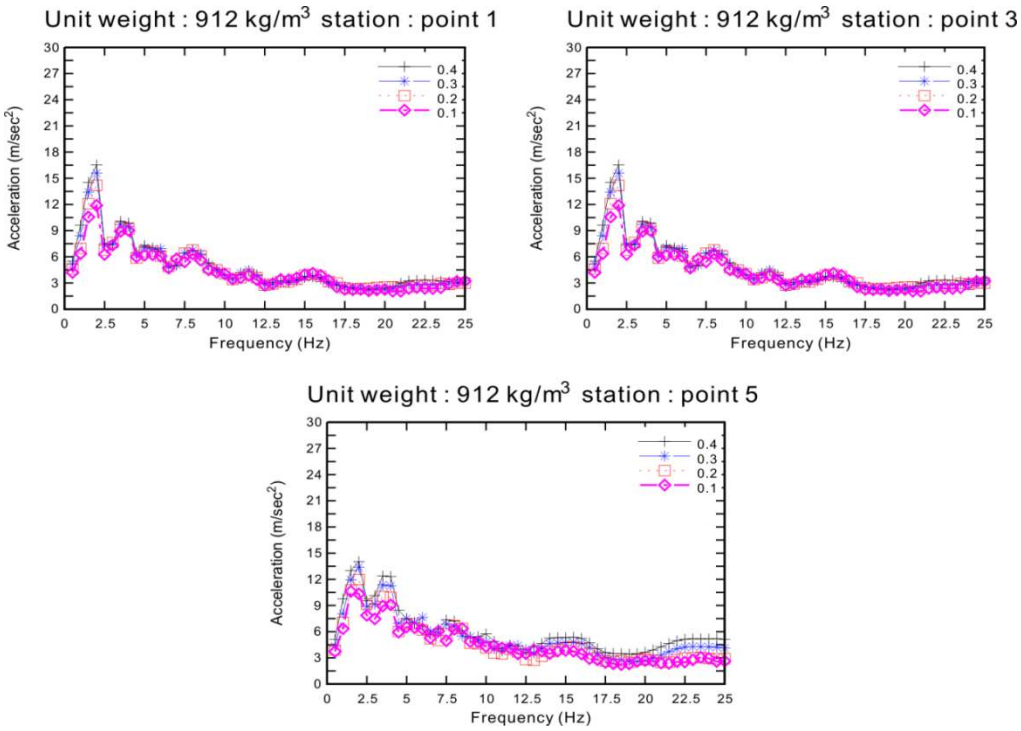

Fig. 43. Floor response spectra of point 1, 3 and 5 during El-centro earthquake motion according to friction coefficient change

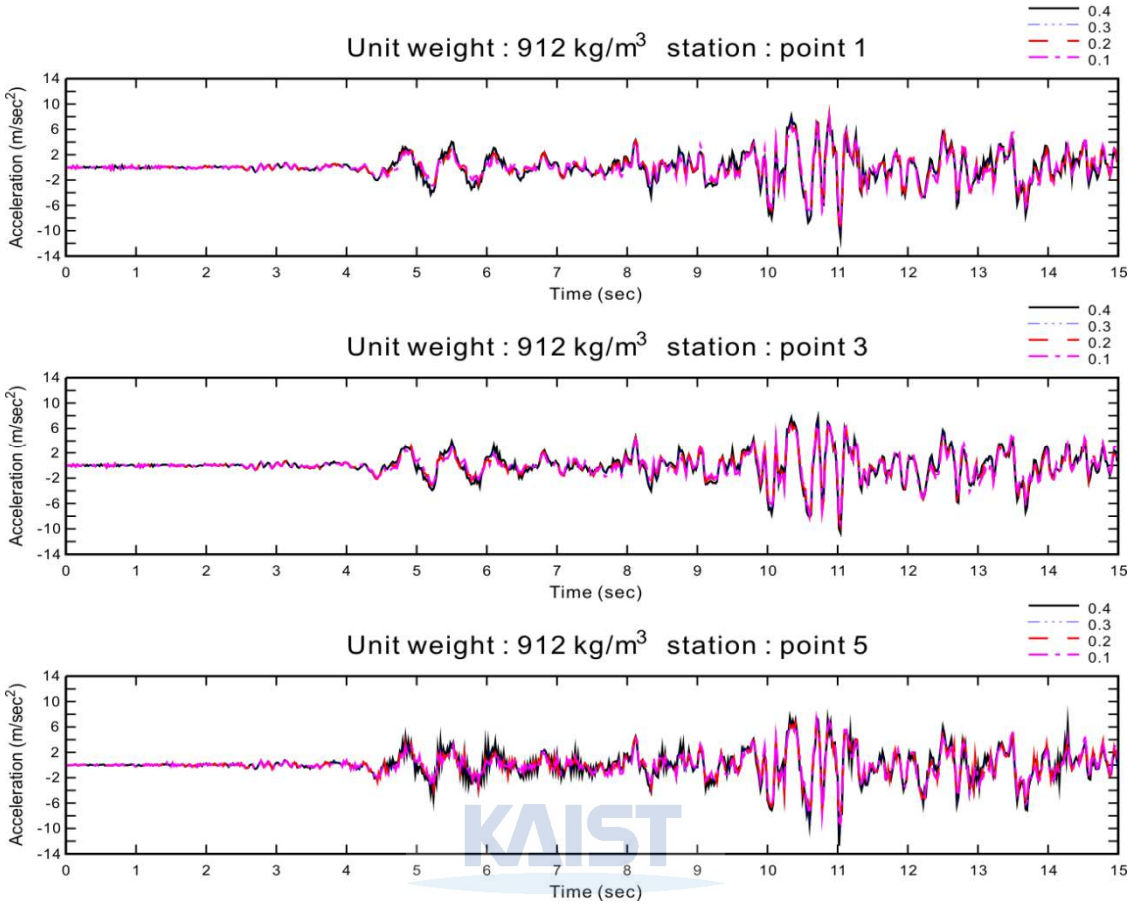

Fig. 44. Horizontal acceleration response in time domain during Tabas earthquake according to change of friction coefficient: point 1, 3 and 5, Unit weight: 912 kg/m3

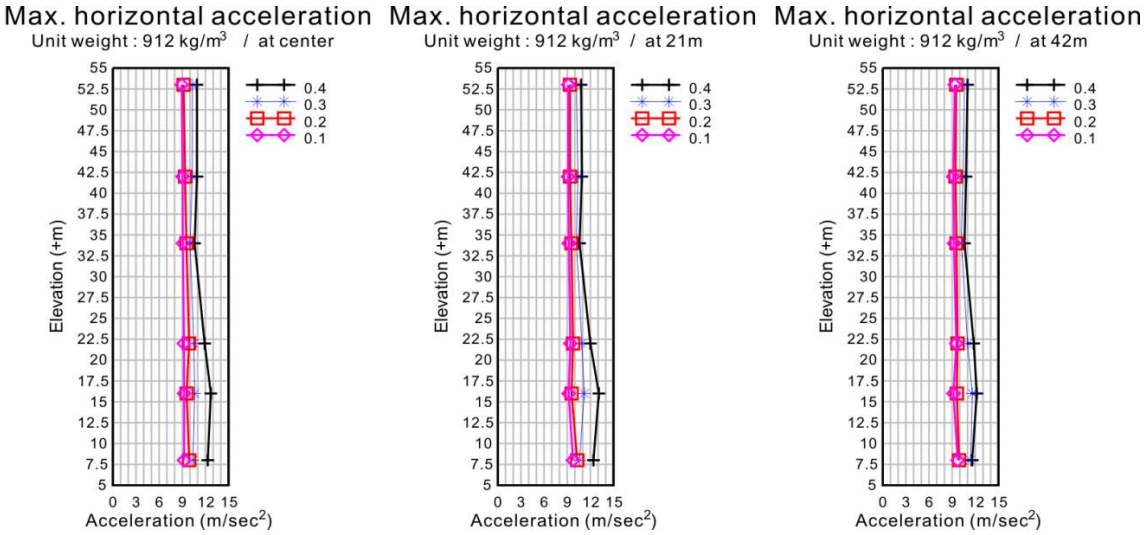

Fig. 45. Comparing absolute maximum horizontal acceleration during Tabas earthquake according to friction coefficient change

Table. 19. Absolute maximum horizontal acceleration according to change of friction coefficient at selected eighteen stations during Tabas earthquake

Unit weight of GBS type ONPP : 912kg/m^3				acceleration unit : m/ sec^2		
Coefficient of friction : 0.4						
Position	53m	42m	34m	22m	16m	8m
0 m	10.9	10.9	10.6	11.9	12.7	12.3
21 m	10.8	10.9	10.6	12	13.1	12.4
42 m	11	10.8	10.6	11.8	12.2	11.6
Coefficient of friction : 0.3						
0 m	10.3	10.3	10	10.5	10.6	10.4
21 m	10.2	10.4	10.2	10.9	11.2	10.6
42 m	10.6	10.4	10.2	11	11.6	11.4
Coefficient of friction : 0.2						
0 m	9.18	9.36	9.54	9.87	9.57	9.89
21 m	9.36	9.37	9.55	9.76	9.56	10.3
42 m	9.53	9.43	9.57	9.69	9.61	9.89
Coefficient of friction : 0.1						
0 m	8.93	9.04	9.09	9.22	9.24	9.24
21 m	9.14	9.13	9.21	9.41	9.19	9.75
42 m	9.35	9.15	9.24	9.54	9.17	9.72

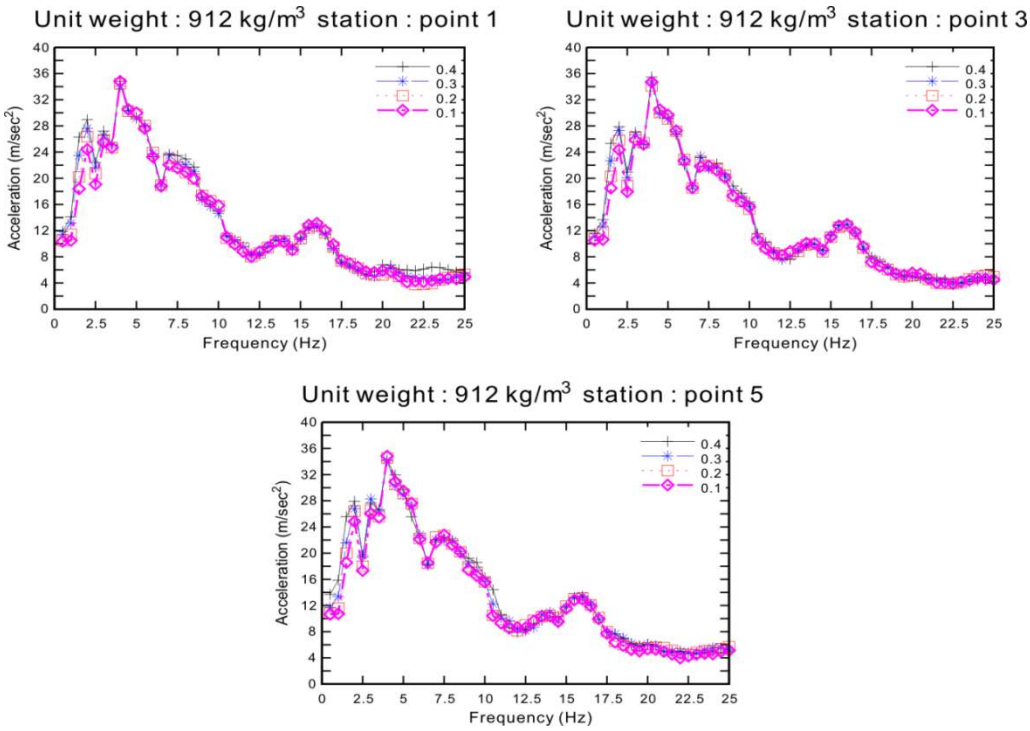

Fig. 46. Floor response spectra of point 1, 3 and 5 during Tabas earthquake motion according to friction coefficient change

Table. 20. Peak responses amplification and dominant frequency region of unit weight change and friction coefficient change during Kobe, El-centro and Tabas earthquake

Point 1									
	Default unit weight : 912 kg/ m^3					Default friction coefficient : 0.4			
Earthquake	Dominant Hz	0.4	0.3	0.2	0.1	Dominant Hz	912	712	580
Kobe	2.50	28.03	26.28	24.12	23.57	2.50	28.03	26.99	24.87
	3.00	21.59	22.43	21.39	19.22	3.00	21.59	22.79	20.15
El-centro	1.50	14.53	13.41	12.10	10.55	1.50	14.53	12.74	9.80
	2.00	16.53	15.59	14.20	11.88	2.00	16.53	14.61	10.23
Tabas	4.00	34.84	34.05	34.45	34.80	4.00	34.84	35.60	35.12
	4.50	30.31	30.38	30.26	30.53	4.50	30.31	30.64	31.81
Point 3									
Kobe	2.50	31.03	29.20	26.51	24.39	2.50	31.03	27.53	24.38
	3.00	24.27	23.16	21.91	20.02	3.00	24.27	22.85	20.29
El-centro	1.50	14.53	13.41	12.10	10.55	1.50	14.15	12.08	9.61
	2.00	16.53	15.59	14.20	11.88	2.00	15.56	13.31	10.01
Tabas	4.00	35.47	34.68	34.12	34.70	4.00	35.47	35.03	35.63
	4.50	29.98	29.78	30.04	30.48	4.50	29.98	31.03	31.65
Point 5									
Kobe	2.50	28.03	26.28	24.12	23.57	2.50	28.03	26.99	24.87
	3.00	21.59	22.43	21.39	19.22	3.00	21.59	22.79	20.15
El-centro	1.50	14.53	13.41	12.10	10.55	1.50	14.53	12.74	9.80
	2.00	16.53	15.59	14.20	11.88	2.00	16.53	14.61	10.23
Tabas	4.00	34.84	34.05	34.45	34.80	4.00	34.84	35.60	35.12
	4.50	30.31	30.38	30.26	30.53	4.50	30.31	30.64	31.81

6.3 GBS bottom Friction verse Fix condition

To verify superiority of seismic performance with GBS bottom friction condition during earthquake, additional dynamic response analysis is implemented in this study which analysis is bottom is fixed to the sea bottom. When the bottom of GBS is fixed to the seabed, the earthquake load is directly transferred to the GBS cause severe damage on the systems and facilities. By using results of friction coefficient change, horizontal acceleration response is depicted in Figure 47, 48 and 49 during Kobe, El-centro and Tabas, respectively. The acceleration reduction effect is clearly observed in the results. As going from bottom to top of the GBS, the acceleration reduction effect is getting clear because in case of bottom fixed to the seabed, sliding motion at the GBS bottom is not allowed and used FE model is not rigid, hence relative motion at the tip of GBS is much bigger than case of friction. It is evident that, bottom friction condition has higher seismic performance than bottom fixed condition. However, the GBS type ONPP is placed in the ocean, so we have to consider the wave load and ocean current in normal state. Fortunately, GBS is a support structure held in place by gravity and the total weight is very heavy, therefore it is less affected by wave load and ocean current. Also, against sever ocean environment, sufficient shear resistance at the base is provided by a corrugated skirt is extended into the seabed and also the skirt is designed to yield under the severe earthquake.

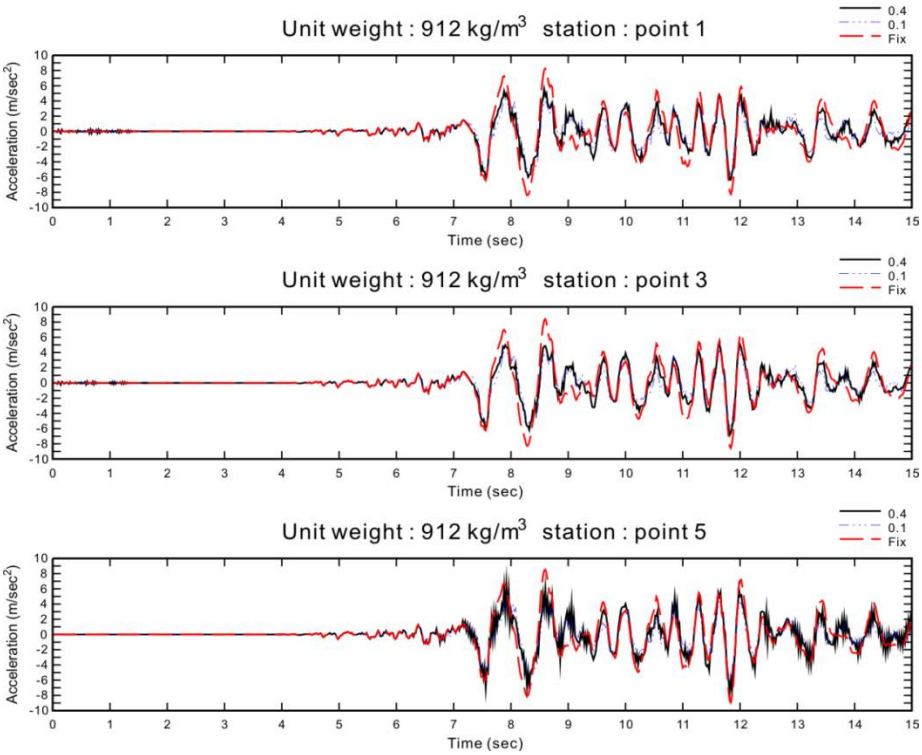

Fig. 47. Comparing of horizontal acceleration response with friction and fix condition during Kobe earthquake.

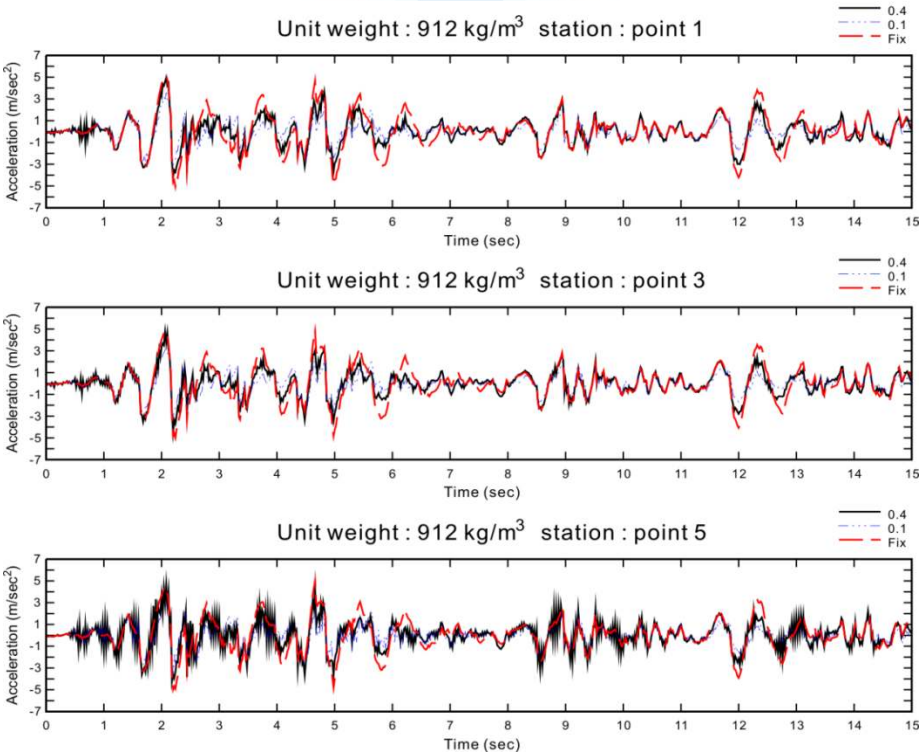

Fig. 48. Comparing of horizontal acceleration response with friction and fix condition during El-centro earthquake.

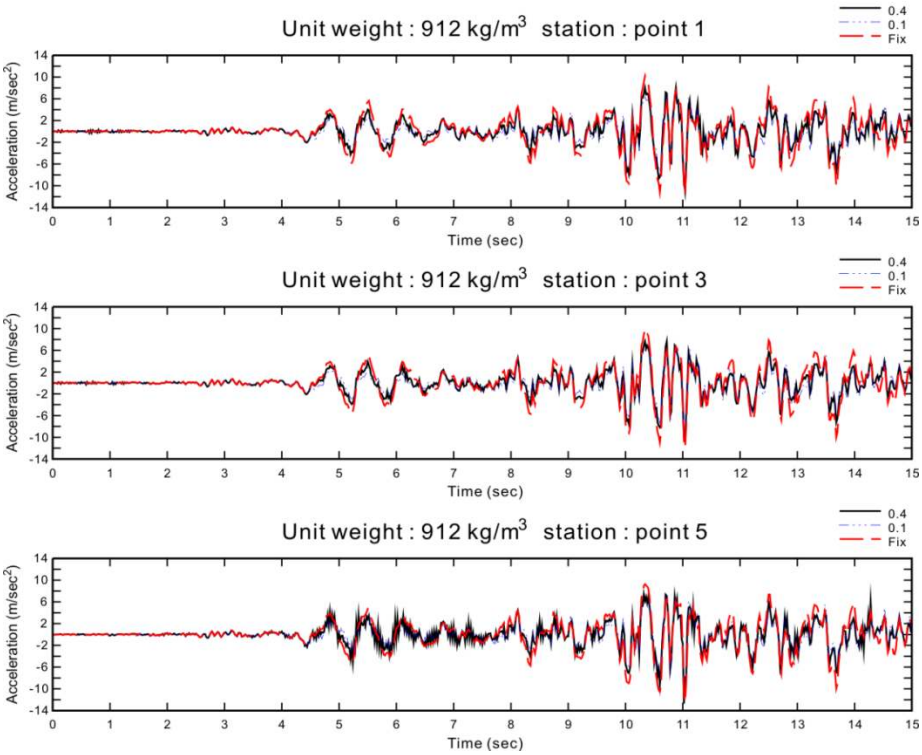

Fig. 49. Comparing of horizontal acceleration response with friction and fix condition during Tabas earthquake.

Chapter 7. Conclusions

The concept design of the GBS type ONPP was developed to satisfy the essential design requirements of nuclear power plants that operate in the ocean to enhance its safety and increase passive nature of the nuclear system. Hence, in this study, several governing design parameters and considerations were proposed from systematic and structural perspectives.

As the supporting and containing structure for the NPP, gravity based structures (GBSs) were chosen due to their features of durability, stability and radiation shielding in ocean environments. In order to mount the APR1400 into three GBS modules, a new general arrangement (GA) is developed and a modular design method is used to separate the overall facilities of the APR1400 into GBS modules. Consequently, the total construction area of GBS type ONPP is reduced by 60% of the original NPP. Furthermore, the symmetric arrangement was achieved by considering the total weight balance of the GBS type ONPP to prevent differential settlement at the seabed. Also, according to the new total GA, the overall length of the pipelines is reduced and the circulating cooling system simplified using seawater as the coolant. By reducing the overall pipeline lengths and simplifying the cooling system, there are expected economic gains.

To enhance the existing emergency passive cooling system (EPCS) and active containment cooling systems of APR1400, a new concept of EPCS was proposed as the emergency passive containment cooling system (EPCCS) and emergency passive reactor-vessel cooling system (EPRVCS). The EPCCS and EPRVCS use the natural differential pressure head between ballast compartment and inside of containment as a driving force for the systems. For instance during a total station black out accident, EPCCS reduce pressure inside of the containment by heat exchangers which using ballast water as cold water source. The ballast water constantly circulates the system to cool down the containment and reduce the pressure inside it to prevent from containment failing. Addition to the EPCCS, EPRVCS is suggested for the case of melting or significant degradation of the reactor to cool and confine of the core melt in vessel through external vessel cooling by ballast water/seawater. The EPRVCS uses ballast water to flood the reactor vessel up to hot legs and cold legs. By the cooling and confinement of core melt in vessel through EPCCS and EPRVCS, a severe accident can be terminated in vessel and thus the release of fission products to the containment can

also be minimized.

In the event of a natural disaster such as an earthquake or tsunami, the GBS type ONPP is safer than land-based NPPs. In case of earthquake, according to control of the GBS weight, GBS bottom is easily decoupled from seafloor and transferred accelerations into the structure is reduced. Consequently, machinery and systems of plant are less damaged during earthquake. When tsunami is occurred, the GBS type ONPP is relatively safer than land-based NPPs because the location of the GBS type ONPP is a few kilometers from shoreline. By using a simple equation, we confirm that the tsunami height at the GBS is 12 meters in case of the Fukushima tsunami. The target water depth is 30 meters, therefore 11 meters freeboard is securing. Consequently, the mounted facilities of the GBS type ONPP are free from green water. Furthermore, for marine collisions, the reinforced concrete double walls of the GBS provide sufficient durability against the impacting load.

Addition to the concept design and safety features of GBS type ONPP, to analyze dynamic response of GBS during selected ground motions, fully coupled analysis of dynamic GBS-seawater-soil interaction with non-linear consideration is conducted in time domain. The Horizontal components of selected ground motion are used in all analysis. The time domain dynamic analyses were implemented by ADINA and FRS approach also used to verify acceleration response in frequency domain. Several cases which according to change of unit weight and friction coefficient were addressed to systematically investigate the effects of acceleration response reduction in the GBS with selected stations.

Firstly, during selected ground motions, the acceleration response reduction effects are investigated according to change of unit weight of GBS. It was shown that the acceleration responses are decreased in time domain and FRS at the important station; point 1, 3 and 5, which point is location of top of GBS, Main operation floor and Steam generator space floor, respectively. Under the harmonic ground motion, almost 50% reduction of acceleration response is observed. However, during real-earthquakes, the reduction effects are not as significant as harmonic ground motion. Besides, at the certain point absolute maximum acceleration of 580 kg/m^3 is bigger than case of 912 kg/m^3. Such phenomenon is occurred by randomness of input ground motion and decreasing of structure inertia which proportional to the mass of structure. The acceleration responses are reduced during ground motion, taken as a whole, but

acceleration response can be increased at the certain point due to reducing of unit weight, especially at the top and end side of GBS. Under the extreme earthquake like Tabas, the effects of acceleration response reduction according to change of unit weight are insignificant.

Secondly, by reducing of coefficient of friction between GBS bottom and seabed, the acceleration responses are reduced also. In contradiction to unit weight change, the reduction effects are more clearly shown in overall analysis because friction coefficient has only effects on the frictional force in contact interface. When we compare the absolute maximum horizontal acceleration and FRS results of both change of friction coefficient and unit weight , the acceleration response reduction effects are almost. In case of Tabas earthquake, like as unit weight change, the reduction effects are not observed in results of acceleration response in time domain, absolute maximum horizontal acceleration and FRS.

Thirdly, to verify seismic performance of pure-friction condition, the case of bottom fixed to the seabed is additionally implemented during selected ground motion. From the suggested results in this study, we confirm that bottom fixed condition has disadvantageous results during earthquake. Such results are more clearly appeared at the top and end side of GBS.

In this study, we used simple box structure for modeling of GBS in seismic performance analysis and verified acceleration reduction effects according to reduction of unit weight of GBS. AS a result of unit weight change, the inertia of whole structure is decreased and acceleration responses of 580 kg/m3 unit weight are bigger than 912 kg/m3 at the top and end side of GBS. In real structure, the unit weight is changed in the ballast compartment only and inner part of GBS is composed of NPP`s structure and facilities. Therefore, to obtain more realistic seismic performance of GBS type ONPP according to unit weight change, we need to develop advanced GBS structure model and NPP model at the same time.

Appendix A. The building and facilities list and GA of the APR1400.

1. Chlorination building
2. Sodium hypochloride holding tank
3. CCW HX building
4. ESW intake structure
5. ESW supply pipe
6. ESW discharge pipe
7. CW intake structure
8. CCW supply and return piping
9. Lube oil storage tank and centrifuge house
10. Co^2 storage tank area
11. Chemical storage tank area
12. Unit auxiliary transformer
13. Main transformer
14. Standby auxiliary transformer
15. Transformer removal rail load
16. Spare main transformer
17. Condensate storage tank
18. AAC D/G building
19. Reactor make-up water tank
20. Hold-up tank
21. Boric acid storage tank
22. Cold machine shop
23. N_2 and H_2 storage cylinder area
24. Fire pump & water/wastewater treatment BLDG
25. Caustic and acid storage tank
26. Fresh water storage tank
27. Demi water storage tank
28. Auxiliary boiler BLDG
29. Auxiliary boiler fuel oil storage tank
30. COND. Tube pull Pit (typ.)
31. GIB tunnel
32. CV cable tunnel
33. Excitation transformer
34. CW intake conduit
35. CW discharge conduit
36. Underground common tunnel
37. Wastewater treatment facility
38. Transformer area pump
39. Spare transformer
40. Cooling tower
41. CW discharge pond
42. KHNP's office area

43. Guard house

44. Intake area

45. Parking area

46. Sanitary water treatment facility

47. Transformer area cable tray tunnel

References

[1] Korea Hydro & Nuclear Power Co., Ltd., Preliminary Safety Analysis Report (PSAR), Revised Vol. 1, 2008.

[2] Knut Waagaard. Design Standard for Concrete LNG Terminal Offshore. *Offshore Technology Conference*, 16207, 2004.

[3] Hannes Ludescher, Jacqueline Naess, Lars Bjerkeli, Detailed Design of a Gravity-based Structure for Adriatic Liquefied Natural Gas Terminal, *Structural Engineering International*, Technical report, 99-106, 1/2011.

[4] Atle K. Haug, Rolf Eie, Knut Sandvik, Aker Kvaerner, and Eiji Aoki. Offshore Concrete Structures for LNG facilities – New development, *Offshore Technology Conference*, 15302, 2003.

[5] Christopher W. Lapp, Michael W. Golay. Modular design and construction techniques for nuclear power plants, *Nuclear Engineering and Design*, 172, 327-349, 1997.

[1] Westergard HM. Water pressure on dams during earthquakes. Trans ASCE 1933;98:418-72.

[2] Oslon LG, Bathe KJ. Analysis of fluid-structure interaction. Adirect sysmmeric coupled formulation based on the fluid velocity potential. Comput Struct 1985;21:219-40.

[3] J. P. Wolf, Non-linear soil-structure-interaction analysis using dynamic stiffness or flexibility of soil in the time domain. EESD1985;13(2):195-212.

[4] ADINA R&D, Inc. Theory and modeling guide, Report ARD 10-7, vol. I; 2010.

[5] Lysmer J, Kuhlamayer RL. Finite dynamic model for infinite media. J ENG Mech Div, ASCE 1969;95(EM4):858-77.

[6] B. Haggblad, G. Nordgern, Modeling nonlinear soil-structure interaction using

interface elements, elastic-plastic soil elements and absorbing infinite elements. Comput Struct 1987;26:307-24.

[7] Arablouei et al. Effects of seawater-structure-soil interaction on seismic performance of caisson-type quay wall. Comput Struct 2011;89:2439-2459.

[8] Ghaemian M, Ghobarah A. Staggered solution schemes for dam-reservoir interaction. J Fluid Struct 1998;12:933-48.

[9] J. W. Chavez et al. Earthquake response of concrete dams including base sliding, EESD 1995;24:673-86.

[10] Ak. Chopra, L. Zhang. Earthquake-induced base sliding of concrete gravity dams. J. Struct Eng. 1991;117:12(22) page.

[11] Cooke HG. Ground improvement for liquefaction mitigation at existing highway bridge. PhD disser. Virginia: Department of Civil and Environmental Engineering, Polythechnical Institute and Sate University; 2000.

[12]Smith IM, Arulanandan K, Scott RF. An overview of numerical procedure used in the VELACS project. In: proceeding of the Numerical Procedures for the Analysis of Soil Liquefaction Problems; 1994. P. 1321-28.

Summary

An offshore nuclear power plant mounted on gravity-based structures and its seismic performance

지진, 쓰나미와 같은 자연재해 발생에 따른 기존 육상원전이 가지는 안정성의 한계를 극복하고 지속적인 원자력발전 사용을 위해 해양원전에 대한 연구가 활발히 진행되고 있다. 본 논문에서는 중력식(gravity-based) 구조물을 이용한 해양원전의 개념설계를 제시하고, 중대사고 시 기존육상원전의 안전성을 향상시키기 위해 해양환경을 활용한 새로운 피동안전 시스템을 제시하였다. 또한 지진 발생시, 중력식 구조물의 동적 특성을 분석하기 위하여, 구조물-유체-지반 상호작용 효과가 고려된 유한요소 모델을 개발하여 상용해석 유한요소 해석 프로그램인 ADINA를 사용하여 그 동적 해석을 시간영역에서 실시하였다. 지진하중 작용 시, 구조물의 동적 특성을 지배하는 구조물의 단위 중량, 구조물과 하부 지반 사이의 마찰계수를 해석 변수로 하여 그 변화에 따른 중력식 구조물의 동적 특성을 비교 분석 하고자 한다.